2017

INVESTIGATION OF THE USE OF 3-D PRINTER PLATFORM AS BUILDING BLOCK FOR RAPID DESIGN OF RESEARCH AND MANUFACTURING TOOL

Handy Chandra
Michigan Technological University, handyc@mtu.edu

INVESTIGATION OF THE USE OF 3-D PRINTER PLATFORM AS BUILDING BLOCK FOR RAPID DESIGN OF RESEARCH AND MANUFACTURING TOOL

By

Handy Chandra

A THESIS

Submitted in partial fulfillment of the requirements for the degree of

MASTER OF SCIENCE

In Computer Engineering

MICHIGAN TECHNOLOGICAL UNIVERSITY

2017

This thesis has been approved in partial fulfillment of the requirements for the Degree of MASTER OF SCIENCE in Computer Engineering.

Department of Electrical and Computer Engineering

Thesis Advisor: *Joshua M. Pearce*

Committee Member: *Zhaohui Wang*

Committee Member: *Gowtham S.*

Department Chair: *Daniel R. Fuhrmann*

Table of Contents

List of Figures

List of Tables

Preface

This thesis consists of two journal articles, one already published and another planned to be submitted. The first article is titled "Open-Source Automated Mapping Four-Point Probe" published in the journal *Materials*. This article is used in Chapter 2 of this thesis and includes contributions from multiple authors. The author's contributions are devising and performing the experiments, designing the hardware and software and analyzing the data. Spencer W. Allen participated in the hardware and software design. Shane Oberloier also helped with the hardware and software design. Nupur Bihari and Jephias Gwamuri assisted in performing the experiment and analyzing the results. Joshua Pearce conceived and designed the experiment, designed the hardware and software, and analyzed the data. All researchers wrote the paper.

The second article is titled "Large Form Factor Open Source FFF-based 3-D Printer for Fabrication of Multi-Cubic Meter Models" and is included in Chapter 3 of this thesis. The article and its experiments are also the work of multiple researchers. The author contributions are designing the hardware and performing the experiments. Nathan Skalsky and Joshua Pearce also designed the hardware and conceived experiments. John Laureto assisted in troubleshooting the hardware. All researchers wrote the paper.

Acknowledgements

I would like to recognize the support of Fulbright Program for making it possible to study at Michigan Technological University and producing this work. I would also like to thank my advisor Dr. Joshua Pearce for his guidance during the whole course of this work. Thank you to my fellow students at Michigan Tech Open Sustainability Technology Lab (MOST) research group for all their help and advice. At last, special thank you to my family for their support during this program.

Abstract

This thesis attempts to show how an open source 3-D printer platform, the self replicating rapid prototype (RepRap), could be used to accelerate the development of research and manufacturing tools. Two projects are shown as examples, both utilizing components of the 3-D printer platform.

The first project is to develop an instrument capable of performing automated large-area four-point probe measurements. A modified RepRap 3-D Printer with a four-point probe in place of the 3-D printer head is utilized as a precision positioning platform. The printer together with custom designed measurement circuit and software performs automated measurement on multiple points on the sample. Three-part experiments were performed to validate the system performance and it was found to be comparable to existing commercial equipment. The developed system is fully open sourced and cost 70% less than manual proprietary systems.

The second project tried to build large size fused filament fabrication (FFF) 3-D printers (2 x 1 x 0.6 meters) by retrofitting an existing CNC machine frame with FFF print head and single board computer running open source 3-D printer controller software. A variety of 3-D object was printed to showcase the printer capability to print simple and complex objects.

The result of both projects is comparable to existing commercial equipment and showed how researchers, engineers and makers could use existing open source 3-D printer platform to accelerate the development of research and manufacturing tools.

Chapter 1

Introduction

3-D printing has been developed since 1980s and was originally intended for rapid prototyping applications. These expensive systems were commonly found only in industry until the replicating rapid prototyper (RepRap) project was founded in 2005. The RepRap project, founded to design 3-D printers that could print out some parts of itself, have made 3-D printing become more common in household and educational institutions. The RepRap project method for 3-D printing was based on patented Fused Deposition Modelling (FDM) by Stratasys which recently expired. The name FDM was trademarked however, and the term fused filament fabrication (FFF) was coined for the process used by RepRap printers. The RepRap project has made 3-D printing become so popular such that an entire community of 3-D printing hobbyists and enthusiasts has spawned and help the open source project become more mature.

RepRap has made all of its designs open source and consists of low cost and printable components, ensuring any average skilled makers and engineers will be able to build them. There are many online communities built around the RepRap printers and its derivatives, ensuring that the users will be able to get the help they need to build, fix, or even extend the capability of their printers. The popularity of 3-D printing has also spawned a lot of new 3-D printing companies, components makers such as hot end makers, filament producers, software vendors and online distributors. The design of many of these open source 3-D printers are modular such that some parts of them can be replaced with one another, such as the bed, hot end, extruder, motion system, or even firmware and software. These printers could manufacture parts with high resolution, down to 100 microns

positioning accuracy such that they are also attractive to be used for other applications, such as for CNC milling. The open source nature of the projects has encouraged modification and expansion of the functionality of the printer such that there are many design variants available, from variations in sizes, materials used, frame constructions, software, and types of axes.

These new developments in 3-D printing technology has the potential to be used to accelerate the designs of new research and manufacturing tools. Researchers and engineers trying to build a new tool that might use some parts of the many variants of these 3-D printers could follow the open source designs instead of building from scratch. These designs are already used and tested by the 3-D printing community and any advantages or drawbacks with particular parts have been found by a lot of 3-D printing enthusiasts. The standard parts for these designs are also usually cheaper and some of them could also be 3-D printed in matter of hours and easily customizable.

This work will investigate several ways to incorporate the open source designs of a 3-D printing platform into the development of new research and manufacturing tools. Specifically, two use cases will be investigated: the use of a 3-D printer as a precise positioning platform for automated mapping four point probe, and the process of converting a large CNC machine to become a large size 3-D printer capable of printing large 3-D objects. The first use case was about how to develop an automated tool for an electrical measurement on multiple points on a thin sheet of semiconductor materials. Existing commercial equipment is very expensive and consists of a precision positioning tool, the four point probe head, and a precision current source and voltage measurement tool. A 3-D printer could be modified to be used as the precision positioning tool with the print head replaced with a four point probe head. Any variant of the RepRap printer could be used and could also be used to measure different sizes of the sample, bigger printers will be able to measure bigger samples. If the positioning tool is broken, it could be fixed easily with the availability of the source and standard parts for RepRap printers.

The second use case is to extend the capability of a CNC machine to be able to 3D print using FFF technology. A CNC machine frame from CNCRouterParts with the size of

2 m x 1 m x 0.6 m already has the existing mechanical and electrical system to position the head accurately within the Cartesian axes. With the selection of a few tested parts from the 3-D printer ecosystem, the machine was turned into a 3-D printer capable of printing large size object. A hot end capable of faster printing speed was selected and an open source 3-D printer controller was used to control the machine. The system will cost less than its commercial counterparts, and easily expandable with many standard or printed parts from the community.

Chapter 2

Open Source Automated Mapping Four-Point Probe[1]

2.1 Introduction

The spreading of the open source movement to science has achieved success as a research accelerator for many disciplines [1]. However, unlike the zero marginal cost of using free and open source software (FOSS), open source hardware development faces challenges arising from manufacturing costs [2]. Significantly, 3-D printing, using low-cost open source self-replicating rapid prototypers (RepRaps), has helped overcome this challenge [3]. The RepRap project has enabled personal production using low-cost polymer-based materials, such as polylactic acid (PLA), acrylonitrile butadiene styrene (ABS) and high-density polyethylene (HDPE) [4], [5]. Scientists and engineers in diverse fields have begun using RepRap 3-D Printers to manufacture the open source digital designs of scientific equipment [6]-[8] including: colorimeters and nephelometers [9], turbidimeters [10], phasor measurement units [11], optics and optical system components [12], liquid auto-samplers [13], medical equipment [14], microfluidic handlers [15], biotechnological and chemical labwares [16]-[18], mass spectroscopy equipment [19], automated sensing arrays [20], DNA nanotechnology lab tools [21], and compatible components for medical apparatuses such as MRI [22]. Digital sharing of designs brings researchers, educators and citizen scientists cutting-edge scientific tools at incredibly low costs [23] compared to commercial options. Open source scientific tools are freely available for governments, universities, corporations and laboratories to reproduce at

[1] The material contained in this chapter was previously published in journal *Materials (doi:10.3390/ma10020110)*

usually between 90% to 99% less than the cost of conventional equipment [6]. Preliminary value analysis [24] shows that research funders (such as NSF and NIH) can see a return on such investments in the hundreds or thousands of percent [25]. To further drive down the cost of scientific research and harness the full capacity of open source design, multiple research applications can be bundled together using an open source 3-D printer itself as a scientific platform [26]. Past work has demonstrated a number of generic fluid handling and analytical techniques using this approach [26] and a 3-D microscope [27].

In this study, this approach is further refined to develop a novel instrument capable of performing automated large area four-point probe measurements of semiconductors for solar photovoltaic (PV) applications in both wafer and thin film form. First, the technical requirements of four-point probe systems are reviewed. Then the designs for the conversion of a RepRap 3-D Printer to a 2-D four-point probe measurement device are detailed for both the mechanical and electrical systems. Free and open source software and firmware are developed to operate the tool and are described. To validate the capability of the circuit to measure a large range of sheet resistances, the device was tested on a wide range of discrete resistors. Then, indium tin oxide (ITO) samples of different thicknesses both pre and post-annealing were tested and the results were compared to a proprietary vendor's four-point probe readings. Finally, 3-D mapping of sheet resistance of ITO samples were performed to demonstrate the device capability to measure non-uniformities in large-area samples. The results are discussed in the context of moving open source hardware development into complex characterization tool space for the semiconductor industry and future work is described.

2.2 Background

The PV industry has continued to grow and accelerate into most nations' energy generation mix. In 2016, global solar installations have continued to grow and are projected to reach 64.7 GW [28], [29]. Despite the growth, PV-generated electricity's levelized costs need to be further decreased to out-compete the highly subsidized fossil fuel-based

technologies and attain tera-watt deployment [30]-[32]. To further reduce levelized costs of solar electricity, more efficient PV devices need to be produced through the use of advanced light management schemes [33]-[38]. Future high-power-conversion-efficiency PV devices must effectively utilize the incident AM1.5 solar spectrum with negligible losses of incident photons into the cell. This requires new novel materials and techniques for the next-generation of solar cells [38], [39]. However, more basic materials research especially on transparent conducting oxides (TCOs) as top contacts for PV devices is still needed. Ultra-thin TCOs, particularly indium tin oxide (ITO) still present some fabrication challenges [40]. There is on-going basic material research into advanced anti-reflection coatings [41], [42] and transparent conducting oxides and electrodes [40], [43], [44]. Improved materials are required to augment performance, functionality, reliability and scalability of PV devices [45], [46] and these materials are compared using resistivity as a core metric.

The most commonly used method to measure resistivity (or sheet resistance) of a thin-film of material is by using a four-point probe device [47]-[57]. The measurement functions by passing a current through the outer two probes, whilst simultaneously measuring the potential produced across the inner two probes. By calculating the ratio of voltage to current, the sheet resistance of the sample can be deduced [47], [48], [57]. The advantage of using the four-point probe method is that the method ignores contact resistance between the probe and material [47], [53], [57], [58]. However, effects due to the geometry of the sample as well as the configuration of the probe often require correction factors to be applied to produce an accurate result [47], [48], [57]-[61]. The need to calculate correction factors can be avoided by employing the dual configuration method, which requires taking an extra measurement with the probes in a different configuration [54], [56], [62], [63]. Reversing current applied to the current probes is also commonly employed to eliminate small offset voltages associated with thermoelectric effects [60].

Sheet resistance measurements are frequently used in PV research as a way to analyze the properties of PV materials during processing. It can be evident from a sheet resistance measurement alone if a substrate will produce a poor PV device and should be discarded. Imperfections during PV processing could result in non-uniform thickness.

Therefore, it is recommended to perform measurements across the entire substrate of the sample [64]. Due to the number of measurement points required by this kind of testing, manual methods tend to be time-consuming. The steps in the characterization process such as: raising and lowering the probe head to different points on the sample, measuring forward and reverse currents, recording the result and zeroing the digital multimeter offset, often requires long time periods to perform. To improve the speed and precision of such testing, automated probe positioning devices can be employed. Automated testing systems available are expensive and proprietary. They are also often inadequate for emerging areas of study such as substrates with complex surfaces. Even if the required modification is minor, the closed-source nature of these device makes such modification prohibitively difficult or expensive [6]. In this study an open source system is described that overcomes these limitations.

2.3. Experimental Setup

2.3.1. Experimental Overview

This work demonstrates a low-cost open source automatic measurement system for sheet resistance. The developed system aims to perform automated measurement of sheet resistance of several points within a sample. Various existing open source hardware and software were utilized to make equipment development faster and more reliable. The system consists of a modified open source RepRap 3-D Printer, a custom-designed measurement circuit, and graphical user interface (GUI) for a computer. A user enters data on the GUI about the geometry of the sample, points on the sample to be measured, current value, and center coordinate of the sample on the 3-D printer coordinate system. The precise center coordinate is not important as it is not possible to precisely position the sample (with 100 micron accuracy) on the print bed. The 100 micron accuracy discussed here is the distance between two points of measurement. Thus it should be pointed out that the uniformity of the conductivity values is in relation to the distance between two or more points on the sample, which are highly accurate rather than an absolute position on the

sample. The GUI software then sends ASCII G-Code to the modified RepRap directly, as it has been pointed out previously that a RepRap 3-D Printers can be used as 3-D motion control equipment for scientific experiments [26]. The RepRap, with a four-point probe head in place of a hot-end, is able to move the probe automatically to several points on the sample with positional accuracy of 100 microns. The GUI software controls the measurement circuit to perform the measurements automatically and saves the results to the computer as a CSV file. The inline four-point probe configuration is used for the system, with outer probes as the current probe and inner probes as the voltage probe. The system is intended to perform measurement with only one four-point probe configuration and will calculate approximate sheet resistance using equation:

$$R_{sh} = 4.532 \frac{V}{I} \quad (1)$$

V and I respectively are voltage measured on the inner probes and current through the outer probes. If the thickness of the sample is defined as t, distance between needles of the probe as s, diameter of the sample as d, and distance of the probe to the edge of the sample as *x*, then Equation (1) is valid only when s/t, d/s, and *x*/s are sufficiently large and the distance between each needle are equal [47], [48], [57], [65]. Several similar systems have been developed [50], [55], [56], but none has tried to develop a system that will automatically measure different points on a sample, nor have the designs been disclosed in a digital format as done here for easy and inexpensive replication by other researchers. The measurement flowchart for the system is shown in Figure 2.1.

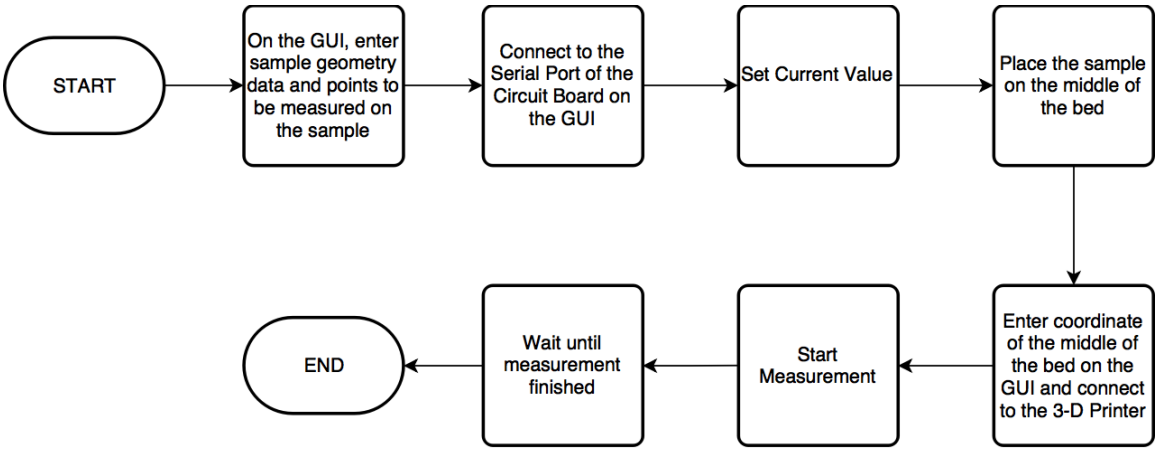

Figure 2.1. Measurement process flowchart.

2.3.2 Equipment and 3-D Motion Control Description

A Prusa Mendel (iteration 1), a RepRap open source 3-D printer, is used to provide precise positioning of the four-point probe on the sample in three-dimensional space. Such a printer has an x-y-z step resolution of 100 microns. A Jandel cylindrical four-point probe head [66], an inline four-point probe, is mounted on the 3-D printer in place of fused filament fabrication printer head. A four-point probe head customized for ITO films with 1 mm probe spacing, 500 µm probe tip radius, and made of tungsten carbide was used in this study [67], [68]. A custom 3-D printed probe head holder was designed to attach the four-point probe head to the printer (Figure 2.2). The designed probe head holder has two parts. The first part is a four-point probe holder used to secure the four-point probe head to the carriage part using two screws (Figure 2.3a). The second part is a carriage part which slides around the x axis smooth rods of the printer and is attached to the toothed belt (Figure 2.3b). The design of the carriage makes it possible for the printer to move the probe assembly around the x axis smooth rods using linear bearings tied with cable ties underneath the holder.

Figure 2.2. Printed four-point probe holder showing mounted four-point probe head.

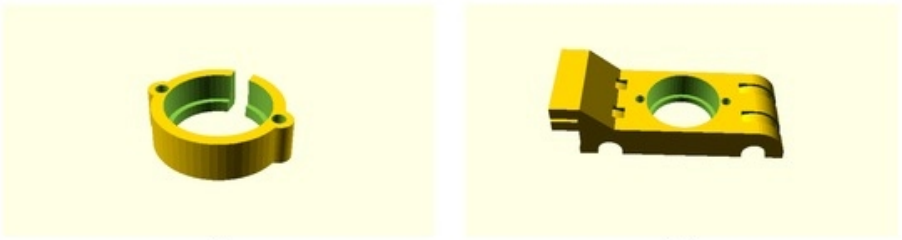

Figure 2.3. OpenSCAD images showing: (a) Probe holder top part; (b) Carriage part x axis mount.

The GUI is able to control the printer directly by sending ASCII G-Code over a USB connection, configured as an emulated serial port. Care must be taken to ensure that there is no z-wobble (change in x and y coordinate when z coordinate is changed) on the printer as this will possibly damage the sample when lowering the probe to the sample. A pair of specimen clips was also 3-D printed to hold the sample in place on the bed so that the sample will not move around and get scratched by the needles of the probe. The bed itself was fixed using springs so that precise z-positioning of the probe is not needed (Figure 2.4). This way the printer will lower the probe head all the way until minimum z-coordinate, and the force of the springs will ensure that the sample will touch the plastic pad on the probe. The sample must touch the plastic pad for proper operation of the probe as recommended by Jandel [66].

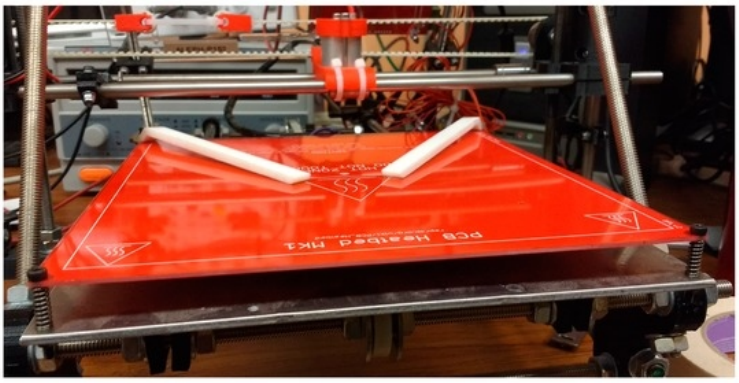

Figure 2.4. 3-D printer bed fixed with springs and a pair of printed specimen clips (white).

2.3.3. Open Source Measurement Circuit

The measurement circuit is designed with the aim to be a low-cost open source alternative to the more expensive commercialized equipment. As such, many design decisions are based on providing sufficient accuracy with low-cost hardware. The circuit consists of an adjustable current source, voltage measurement circuit, and an Arduino-compatible microcontroller board as the main controller for rapid development.

2.3.3.1. Adjustable Current Source

Sufficiently large current must flow through the sample so that the voltage generated between the two inner probes will be large enough to measure accurately [58]. Because contact resistance exists between the probe and sample [57], [69], generating sufficiently large current means a large voltage drop will also exist on the contact resistance, potentially exceeding the current source voltage compliance. Because of this a current source with ~48 V voltage compliance is designed as seen in Figure 2.5. An operational amplifier ADA4522 from Analog Devices is chosen because of its 55 V operating voltage, required for designing a high voltage compliance current source, and

because of its low bias, low offset, and zero drift, which are required for accurate sensing and amplification of small voltages [70], [71].

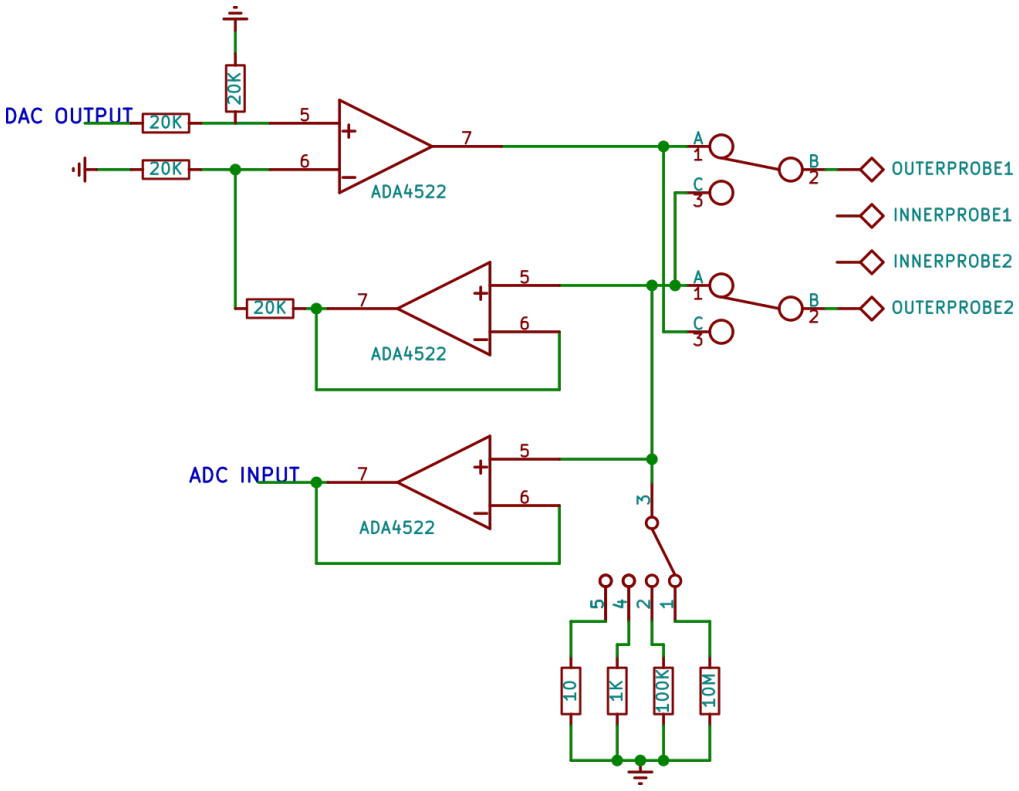

Figure 2.5. Current source circuit.

Another design requirement is that the current source must be adjustable across a large range; from nanoampere to miliampere to accommodate a broad range of sheet resistance values. The combination of digital to analog converter (DAC) and a set of four resistors will allow a wide range of current value to be set. A difference amplifier circuit [72] will set the voltage across the set of four resistors to be the same as the analog voltage from DAC. Switching the active resistor together with changing the analog voltage value will allow a current range from 10 nA to 10 mA.

A set of four single-pole, single-throw (SPST) reed relays [73] are chosen to switch the set of four resistors because they feature a very low ON resistance and have virtually

no leakage current, which minimizes error in the measurement. Another set of reed relays was also added to provide the capability to reverse current during measurements.

The actual value of current needs to be known for the calculation. Because of the limited capability of the current source circuit to set exact value of current, a feedback mechanism is introduced where the analog voltage on the set of resistors is read back by an analog to digital converter (ADC). The ratio between the analog voltage and the value of resistor will give the actual value of current. However, because of parasitic resistance due to ON resistance of the relay and current leakage due to input bias of op-amp (Figure 2.6), a slight error will occur when measuring the actual current. Current leakage may also occur because of insulation resistance of cables, probes, and the test fixture [74]. In general, the lower the current value needed to measure a sample, the greater the inaccuracy will be because a low current value is more susceptible to external noise. A simple RC low pass filter was added on the input of ADC to reduce signal noise when measuring the current value. Finally, the circuit is also capable of disabling the current source by setting the DAC voltage to zero. This is required when lowering the probe to prevent arcing between the probe and the sample, which could damage the sample and shorten the lifetime of the probe.

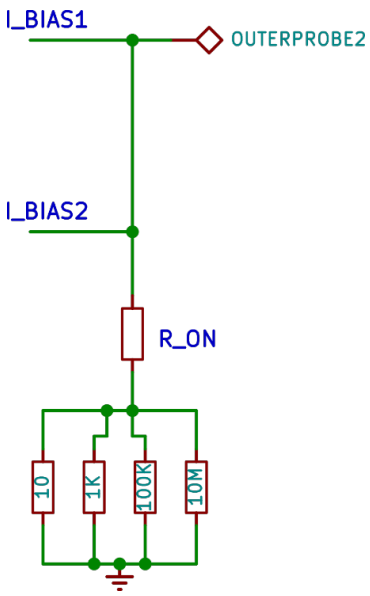

Figure 2.6. Parasitic resistance and leakage of current source circuit.

2.3.3.2. Voltage Measurement Circuit

The voltage measurement circuit should be able to measure small voltage differences accurately and should draw very little current. Thus, an instrumentation amplifier circuit [75] is designed with selectable gain between 1 and 200 by switching a set of two resistors using a reed relay (Figure 2.7). A differential ADC on the Arduino-compatible board is used to measure the output of instrumentation amplifier circuit with respect to a voltage V_{mid}, which is half of the ADC reference voltage. This makes it possible to measure voltage on the inner probe for both forward and reverse current configuration.

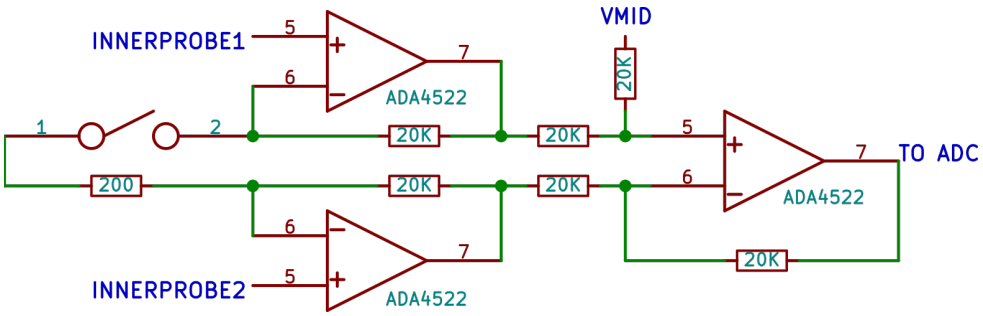

Figure 2.7. Instrumentation amplifier circuit.

Imprecise values of the gain resistor, finite ON resistance of reed relays and imprecise matching of resistors in the instrumentation amplifier circuit will contribute to gain error in the circuit. To minimize the error, a 0.01% tolerance resistor is used in the circuit. An RC low pass filter was also added on the output of this circuit to reduce noise on the measurement results.

2.3.3.3. Main Controller

Teensy 3.2, an Arduino-compatible board powered by a Freescale MK20DX256VLH7 chip (32-bit ARM microcontroller), was chosen as the main controller for the circuit. The need to develop low-cost open source equipment and time constraints during the development influenced the decision to use this board. The chip provides on-board 12-bit DAC, 16-bit single-ended and differential ADC which is needed for the current source and voltage measurement circuit, respectively. Arduino is also suitable for rapid prototyping because of readily available libraries and boards [6], [76]. Initially, the circuit was prototyped on a breadboard to verify the circuit operation. The printed circuit board version of the circuit was designed using KiCad EDA [77]. Next, the designs were fabricated and assembled into a fully assembled circuit (Figure 2.8). All of the KiCad schematics and printed circuit board files needed to make both a breadboard circuit and printed circuit board version are available at the Open Science Framework [78].

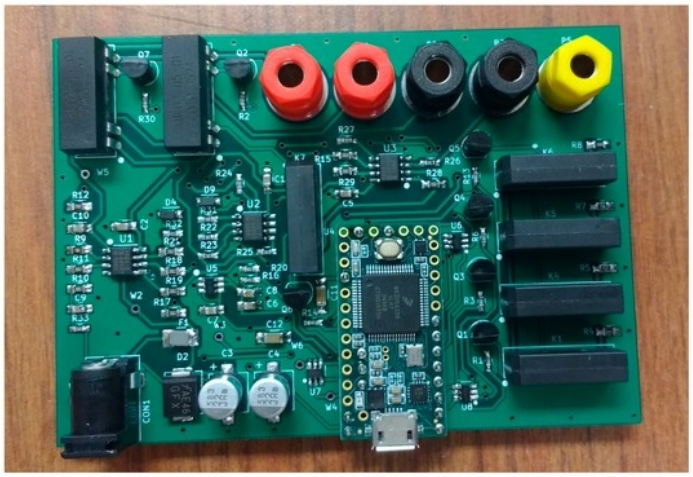

Figure 2.8. Assembled open source printed circuit board for four-point probe measurements.

2.3.4. Firmware

A custom firmware was written using the Arduino Integrated Development Environment (IDE) and open source libraries for rapid development. The firmware was designed to receive and reply to commands over a USB connection via GUI software running on a PC. Several features of the firmware include: detecting whether samples are connected to the probes, disabling and enabling the current source, automatically detecting suitable current levels for the connected sample, automatic gain setting for instrumentation amplifier, switching forward or reverse current configuration, and also include a digital low pass filter to reduce noise from the measurement results. The auto current feature will select among these current values: 10 nA, 100 nA, 1 μA, 10 μA, 100 μA, 1 mA, 10 mA, that will generate sufficient voltage between the two inner needles when the sample is touching the probe. The firmware is released under a GNU FDL and can be downloaded from [79]. An attempt to reduce the effects of ON resistance of the reed relay is done by adding the value of measured ON resistance into the firmware calculation.

2.3.5. Software and Graphical User Interface (GUI)

The Java swing toolkit, included in the Java Development Kit [80], is used to develop the GUI because they are platform independent and the GUI could be rapidly generated using tools such as WindowBuilder [81]. The GUI could be designed easily using drag and drop methods, and uses a “what you see is what you get” (WYSIWYG) interface of this open source tool. The finished user interface is shown in Figure 2.9.

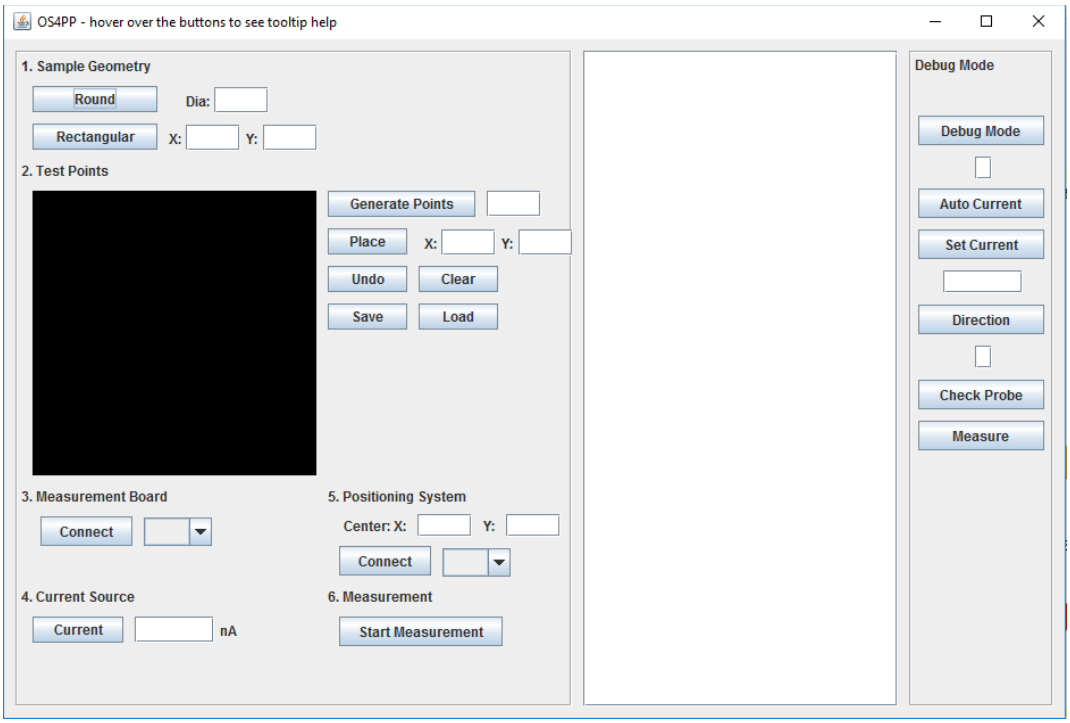

Figure 2.9. The graphical user interface (GUI) for open source four-point probe (OS4PP) software.

The user interface is divided into three parts: the measurement settings in the left part, text display in the middle part, and an area to debug commands on the right. The measurement settings are straightforward to use, with numbered steps to follow. Users can enter which point on the sample to measure manually or it could be generated automatically. The measurement process and result can be seen in the text display. The software will automatically turn off the current source before lowering the probe head, and then turn it on again after touching the sample. This is done to prevent arcing between the needles and the sample. The software will control the printer to move the probe head through all programmed points. The coordinate of each point, current and voltage measured is stored as a CSV file as the measurement process is ongoing and can be exported after the characterization process is complete. The GUI is released under GNU FDL and can be downloaded from [78], [79].

2.4. Validation

The developed system is designed to be able to measure sheet resistances of various materials, but depending on the probe and material itself, a large contact resistance could occur. The current source would be unable to supply enough current to generate sufficient voltage between the two inner probes due to a limited compliance voltage. Therefore, to validate the capability of the circuit to measure a wide range of resistances, contact resistance can be avoided by measuring different values of discrete resistors. The test configuration can be seen in Figure 2.10. It should be noted that the resistors do not need to be equivalent in Figure 2.10. The method is only measuring the central resistor, R2.

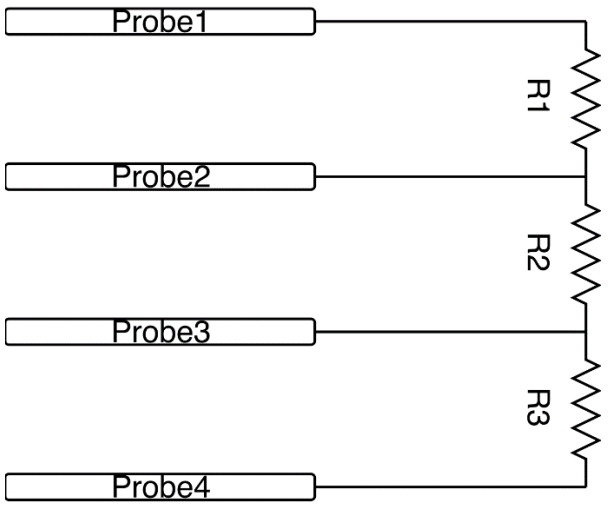

Figure 2.10. Discrete resistor measurement circuit.

The value of the resistors for validation are 10 MΩ, 1 MΩ, 100 KΩ, 10 KΩ, 1 KΩ, 100 Ω, and 10 Ω. Current source values are set so that sufficient voltage is generated on the resistor. The measured value using the open source four-point probe circuit is compared with the measured value by a Fluke multimeter model 187 whose accuracy specification is up to 1% + 4 for resistances up to 32 MΩ. The comparison verifies that the circuit is able to measure a wide range of sheet resistances, namely from mega ohm range to tens of ohm.

The intended purpose of the developed system is to measure ITO samples. To this effect, the second validation was performed on a set of ITO samples, which are: Jandel ITO reference sample 12.58 Ω/square and three 50 nm thick ITO samples on glass annealed for 10, 20, and 30 min respectively using UHP forming gas (FG) (95% N_2/5% H_2 from air gas) in a sealed (by vacuum coupling components) quartz tube inside a tube furnace. The annealed samples were deposited on glass substrates using RF sputter deposition techniques as described in [40]. The measurement results from the open source four-point probe are then compared to results obtained from two other commercial four-point probe systems (Jandel RM3 Test Unit with Lucas Lab probe station, and a system comprising of separate Keithley Current Source Model 220 and Keithley Multimeter Model 196). The measurement method for the three films were performed by measuring 30 random points throughout the samples. Standard deviation from each sample is also calculated to show the range of thickness variation of the film sample.

The last validation is to perform automated measurement on multiple points on the reference sample and also on the three annealed 50 nm samples. There were 100 points automatically generated on the GUI and distributed uniformly over an area of 40 × 40 mm^2 located at about the center of the reference sample. To avoid correction factor calculations, the points were made to be at least 10 probe spacings away from the edge of the sample, with the probe spacing being 1 mm. Because of the small size of the three annealed samples, only 40 points were measured over an area of 10 × 10 mm^2. The measured sheet resistance values are then used to map the sample surface using surface plots to show the degree of variation in film uniformities over the sample surface.

2.5. Results and Discussion

The full OS4PP system consisting of modified printer connected to the measurement circuit can be seen in Figure 2.11.

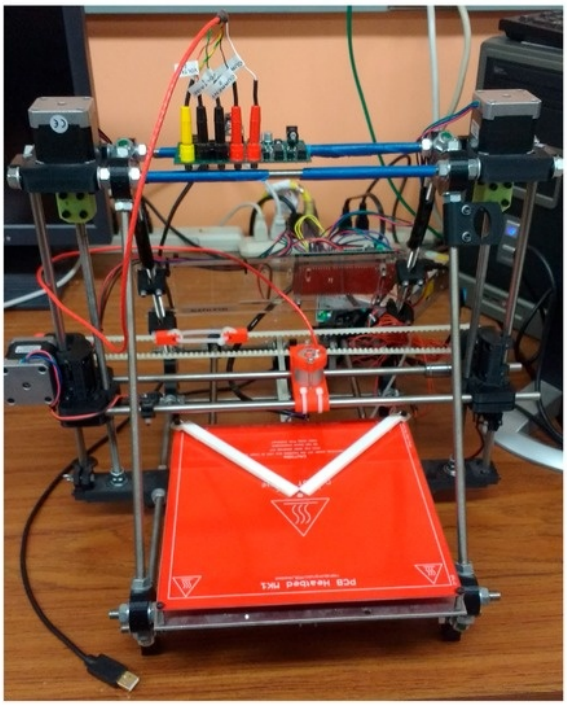

Figure 2.11. Modified 3-D printer with custom measurement circuit for OS4PP measurements.

The results of the resistor measurement using the OS4PP system and fluke multimeter can be seen in Figure 2.12. The comparison of measurement results of resistors from 10 to 1 MΩ show errors of less than 1%, while measurement result of 10 MΩ resistor shows an error of about 2%. Measuring 10 MΩ resistor requires a very low value of current, on the order of nanoampere, which makes it more susceptible to noise. Furthermore, high-resistance materials do not allow the charge to decay quickly, resulting in unstable measurements.

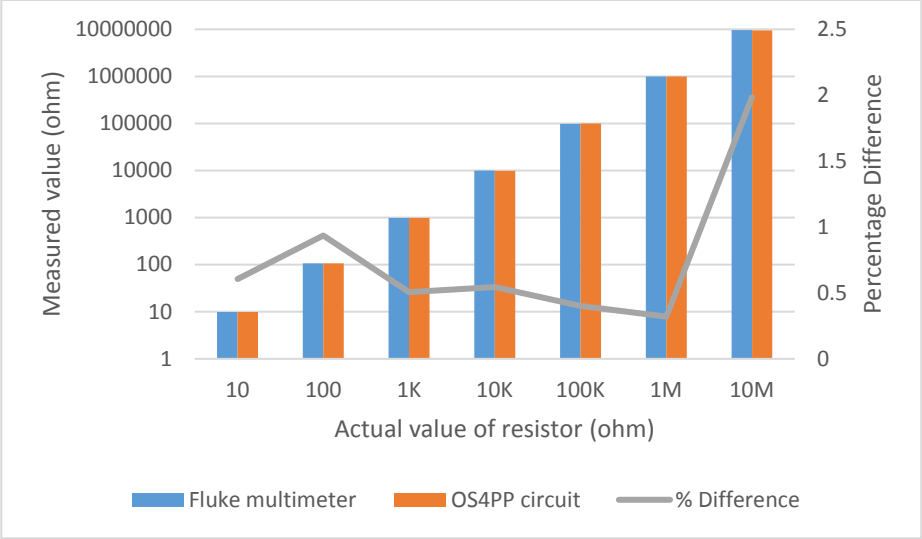

Figure 2.12. Comparison of measurement results on discrete resistor.

Table 2.1 shows measurements of ITO samples using the three different equipment types. The results measured from three different equipment/systems show varying amounts of standard deviation due to non-uniform variations in ITO film thickness and different measurement points for each sample. The standard deviation for sheet resistance measurements for the reference samples using different systems is observed to be consistently lower, and the sheet resistance values can be considered to be constant and within the margin of error. This cannot be used as a comparison for accuracy, because the samples are non-uniform and the choice for each points for different equipment also vary. The results presented in Table 2.1 show the effect of annealing time on the resistivity of ultra-thin ITO films and are in agreement with results presented in refs [40], [45]. There is an observed general trend of decreasing R_{sh} with increasing annealing time and the lowest R_{sh} value is attained for films annealed for 20 min beyond which the R_{sh} is observed to increase. Despite showing a high standard deviation value for the 50 nm film annealed for 30 min, the results indicate that all measured values are within the same order of magnitude when the three types of equipment are compared. In summary, the OS4PP system (with ITO optimized tips) is comparable with the commercial four-point probe systems.

Table 2.1. Measurement results of several indium tin oxide (ITO) samples on different equipment.

Sample	OS4PP		Jandel		Keithley	
	Rsh (Ohm/sq)	**Std Dev**	**Rsh (Ohm/sq)**	**Std Dev**	**Rsh (Ohm/sq)**	**Std Dev**
R. Reference Sample	13.308	0.49	13.09	0.85	13.304	0.27
A. 50nm ITO annealed 10 min	171.86	11.79	182.36	15.21	176.08	8.4
B. 50nm ITO annealed 20 min	110.76	7.33	113.42	9.18	111.8	5.83
C. 50nm ITO annealed 30 min	142.84	27.76	177.52	42.79	159.07	15.9

Figure 2.13 shows automated measurement results using the OS4PP. A point in coordinate (10.91, 29.09) on the ITO reference sample had a sheet resistance value 27.2 Ω and had to be rescaled. There were visible surface defects on these samples because of repeated experiments which explains why a point on the reference sample had very high sheet resistances compared to the rest of the points. Also there is a possibility that annealing the film for 30 min might have triggered some transformation in the morphology of the film resulting in area on the sample surface having isolated islands due to agglomeration. The high value of standard deviation is also seen while using the commercial systems, further proving that inconsistencies in the thin film may have caused the OS4PP to record real values.

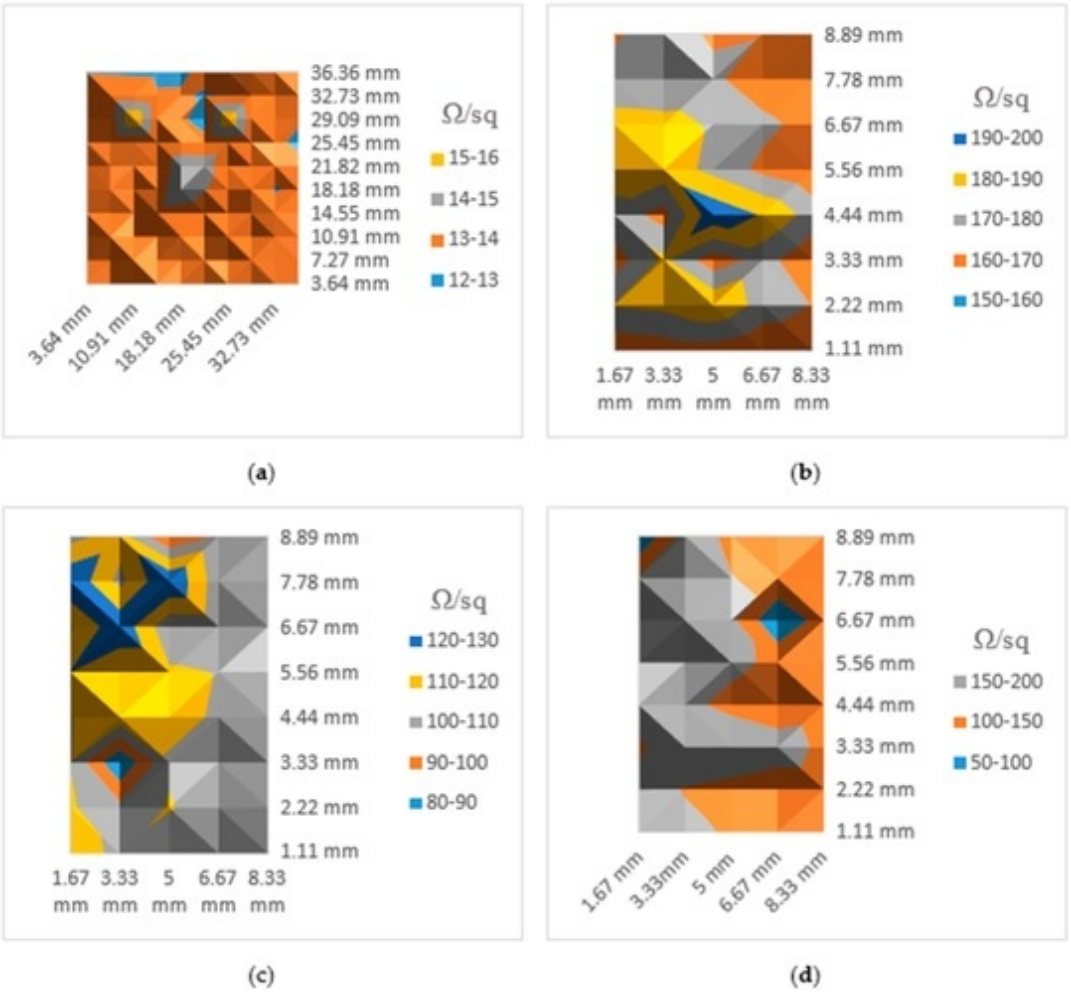

Figure 2.13. Results of automated sheet resistance measurement (Ω/sq) using OS4PP: (a) Reference sample; (b) 50 nm ITO annealed 10 min; (c) 50 nm ITO annealed 20 min; (d) 50 nm ITO annealed 30 min.

The automated measurement results also confirm results in Table 2.1, where standard deviation in Table 2.1 is proportional to the uniformities of the sample. Samples in Figure 2.13 (a) and 2.13 (c) do not vary as much as the other two, which is why their standard deviation is lower. The measurements are also very sensitive to dust, dirt, or other foreign substances on the sample. Generally, the same measurements are taken multiple times to make sure the results are not affected by bad contact to the sample. Normally such tests would be done in a clean room directly after deposition, thus removing this source of

error. However, the lack of an in situ sheet resistance measurement system post-deposition gives valuable information. Further, this tests for film integrity over long periods of time. It is known that oxygen absorption in ITO films affects conductivity and transparency [82], [83]. Hence, there is a need for an automated system that can measure this change in sheet resistance ex situ without the need for repeated intervention by a skilled technician. Further, the automated nature of the OS4PP ensures that the same point is measured each time for longitudinal studies. This mitigates the disadvantage of commercial equipment where the probe is manually placed and is subject to operator error.

Taking the results of three validations into account, the developed open source system performs well in comparison to other commercial systems and could be used as a substitute to conventional equipment in applications requiring automated measurements of large number of points on the samples. The resistor validation shows how accurate the system could be, less than 1% error for sheet resistances smaller than 1 MΩ. The OS4PP performs better at measuring lower values of sheet resistances because higher value of current could be used for these samples, increasing the signal to noise ratio. Actual sample measurements are complicated by variability in contact quality between the probe and samples, and as such taking multiple measurements and averaging them is recommended. The developed OS4PP is compared to Jandel four-point probe system in Table 2.2 to show the differences in features, capabilities, and costs. Calculating the total cost of probe head, circuit, and 3-D printer shows a 73% reduction in cost from the manual commercial four-point probe. It should be pointed out here that the area the OS4PP can cover is much larger than the Jandel as can be seen in Table 2.2. In addition, and perhaps most importantly, the OS4PP is automated with x and y positional accuracy of 100 microns while the more expensive commercial system is not automated and involves manual placement of the sample. The open source nature of this project also allows researchers to study how the tool works and modify it according to their specific research needs. As this project consists of several open source hardware and software projects, any part could be modified, replaced or repaired if damaged.

Table 2.2. Comparison of commercial proprietary machine with OS4PP.

Component	Commercial Machine	Open-source OS4PP
Probe	Jandel macor probe head	Jandel cylindrical four point probe head
Measurement Unit	RM3 test unit	Custom measurement circuit
Mounting Stand	Lucas labs S-302-4	RepRap Prusa Mendel i1 with custom probe holder
Source	Closed source	Reprap project + osf.io
Cost	$1600 probe head + $3200 RM3 + $2500 S-302-4 = $7300	$1600 probe head + $130 circuit + $250 RepRap = $1980
Maximum Wafer Size	4” circular	8” x 8” square
Accuracy	0.3 % (high sensitivity mode)	1 % (< 1M ohm sheet resistances)
Positioning Resolution	Manual sample placement by hand	100 microns X and Y accuracy
Multiple Measurement	Manual	Automatic

There are several ways the OS4PP can be improved. The accuracy of the tool depends on how accurate the set of four shunt resistors are and how small the effects are of the ON resistance of the reed relay. Actual sample measurements could vary depending on the contact quality from the probe to the samples and also because of dust and foreign substances on the samples. In general, good ITO films have lower sheet resistance values (a few kΩ/square or less), hence such films can be characterized with much greater accuracy. There is, however, the need to continue improving the performance of the designed custom measurement units. Proper steps must be taken to minimize the effects of electrostatic fields, leakage currents and temperature among others. Electrostatic shields can be built to enclose the sensitive circuitry and the cabling in the circuit. Substituting the unshielded reed relay into a shielded one could also help reduce the noise in the measurement. Using good quality insulators, reducing humidity, and using guarding may minimize the effects of leakage current [74]. Minority/majority carrier injection is also a problem that could be minimized by keeping the voltage generated between the two inner needles low [74]. Finally, a more accurate ADC will be needed to sense low voltages

accurately. Additionally, a calibration method might be required to eliminate the effects from finite ON resistance of relays.

2.6. Conclusions

Research in basic electronic materials for solar photovoltaic cells and other applications is hampered by the costs associated with electrical measurement of the materials. In this paper, an open source methodology has been applied to electrical conductivity measurements to solve challenges in basic materials research by reducing the cost required for scientific characterization equipment. Digital sharing of the designed scientific equipment combined with open source 3-D printers have made such open source scientific equipment easier and faster to develop. The open source nature has also made it easier to customize the equipment for different applications or fixing the equipment when there are problems. In addition, the open source documentation is all readily available so researchers will know exactly how it works, and there is no ambiguity as to how measurements are made.

The use of the self-replicating rapid prototyper (RepRap) printer, together with a custom measurement circuit, have been investigated to provide a low-cost, open source alternative to expensive automated sheet resistance measurement equipment. A four-point probe head has been installed in place of a 3-D printer head and controlled with software. A custom-designed measurement circuit together with graphical user interface (GUI) software were developed to measure sheet resistance of ultra-thin indium tin oxide (ITO) film samples. The validation shows that the circuit could measure sheet resistances smaller than 1 MΩ with less than 1% error. The results indicate that all measured values are within the same order of magnitude when compared to two proprietary measurement systems. This compares favorably with proprietary commercial systems. In addition, the open source four-point probe (OS4PP) developed here automates the measurement of sheet resistivity. The results of 3-D mapping of sheet resistance of the ITO samples successfully demonstrated the automated capability to measure non-uniformities in large-area samples.

This is generally done manually when using manual four-point probe stands, which has far less positional accuracy than the 100 micron resolution shown here. The automation process can help in film surface mapping in a short period of time thereby promoting the efficient utilization of resources. In conclusion, the OS4PP system, which costs less than 70% of manual proprietary systems, is comparable electrically while offering automated 100 micron positional accuracy for measuring sheet resistance over larger areas.

Chapter 3
Open Source Large Form Factor FFF-based 3-D Printer for Fabrication of Multi-Cubic Meter Models[2]

3.1 Introduction

Although additive manufacturing (AM) has been well established in industry [84], 3-D printing did not become a popular topic for major economic impact [85] until the open source development of the RepRap project [86]-[88]. This is because the RepRap 3-D Printer has enabled true distributed digital manufacturing even at the household level [89]-[91]. It enables prosumers (producing consumers) to fabricate their own products for less money than it costs to purchase them conventionally [92]. Such desktop 3-D printers can be used for a wide range of applications from consumer products [93] to high-end scientific equipment [94]-[96]. In addition, they can be used to print appropriate technologies for sustainable development [97], [98]. However, one of the limitations of these printers is their relatively small volumes for printing out large scale parts for applications like farming [99] or automotive parts [100]. Currently, Fused Filament Fabrication (FFF) 3-D printers capable of printing more than a single meter cubed are expensive proprietary equipment such as Big Area Additive Manufacturing System (BAAM) [101], BigRep ONE [102], The BOX [103], Hori Z1000 [104], ErectorBot [105], Leapfrog Xcel [106], 3D Demonstrator [107], AM1 [108], Builder Extreme [109], X1000 [110], Cheetah [111], 3D Platform Excel [112], ProtoCentre 1M [113] and The Cronus [114]. These printers could cost from around ten thousand for Cheetah to millions of dollars for BAAM. The capabilities of these printers

[2] The material contained in this chapter is in preparation for submission to a journal

also vary, from very large printer capable of printing multiple kilograms per hour, multiple gantry, multiple print head and nozzle, enclosed chambers, multiple axis manufacturing, specialized pellet extruder, and very precise layer resolution. These large size printers have been used to print a variety of big models whether for prototyping or for finished products. One example is the BAAM has been used to print car frame, kayak, table, chair, and miniature models [115]. Some machines have mixing extruder and might be of interest to researchers for trying out new materials such as printing magnets [116].

One of the reasons 3-D printing became popular outside of industry and widely available is because of the open source nature of the RepRap project which create a support ecosystem for those printers [117]. The available documentation, community support, standard and widely available parts enables makers and researchers to fix any problem, modify and extend the printer functionality [118]. The closed-source nature of those commercial big size 3-D printers make it difficult for makers and researchers to extend or modify the mechanical design, electrical design, or the software for their own projects [95], [119]. Thus, to encourage rapid innovation in large areas 3-D printing there is a need to extend the selection of open source 3-D printers to include large size 3-D printers.

To fill those needs, this work discusses the build implementation of a large-scale (2 meter length x 1 meter width x 0.6 m height build size) FFF style open source 3-D printer. The printer was constructed by modifying a large CNC machine system from CNCRouterParts [120]. The existing x and y axis motion system were used, and a new z axis movable bed was added instead of the moving CNC spindle head. A custom machined 3-D printer head is installed in place of the previous CNC head. The assembled 3-D printer head consists of tool holder, direct extruder, hot-end holder and hot end. The hot end can be changed, allowing the use of variety of hot-ends. Most of the existing CNC electronics were used, except the controller board. A single board computer is used as the controller board and additional main interface circuit board was designed to interface with the existing electronics. An open source printer controller, Franklin, was selected to control the printer. The finished system was used to print several objects from small to large to verify its functionality to print simple and complex 3-D models.

3.2 Overall Implementation and Design

The printer was designed with three main objectives: 1) to be able to print large size 3-D models with sufficient accuracy, 2) to fill the need for an open source large form factor FFF 3-D printer, and 3) to be able to switch the function of the machine easily by switching the tool head. A CNC machine frame has the toughness and stiffness for accurate positioning across all length of the axes, and for supporting heavy mechanical parts, large printer bed (110kg) and large 3-D printed parts. The overall construction of the printer can be seen in Figure 3.1.

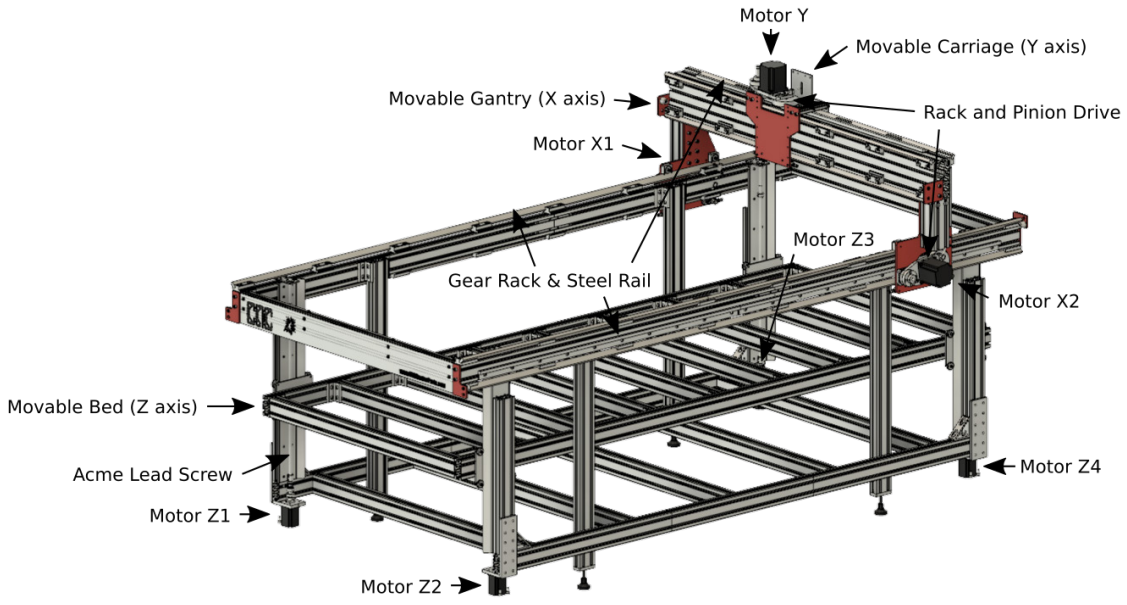

Figure 3.1. Open source large form factor 3-D printer.

3.2.1 Mechanical Design

The frame of the machine was constructed from 4080 T-slot aluminum extrusion to be the shape of a table with four legs and leveling mounts at the base of each leg (Figure 3.2). A patented linear guide device by CNCRouterParts [121] consisting of a clamp holding a steel bar at an angle is placed along the length of x and y axis (Figure 3.3). The linear guide device will allow the gantry and head carriage to slide using v-roller bearing (Figure 3.4). Two stepper motors mounted on each leg of the gantry are used to drive the gantry along the x axis, and one stepper motor mounted on top of the head carriage is used to drive the carriage along the y axis. A tool holder is fixed to the head carriage to hold the extruder (Figure 3.5).

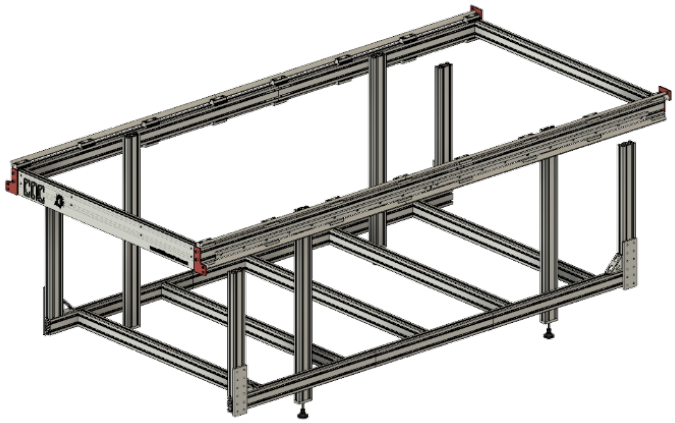

Figure 3.2. Base Frame.

Figure 3.3. Linear guide.

Figure 3.4. v-roller bearing.

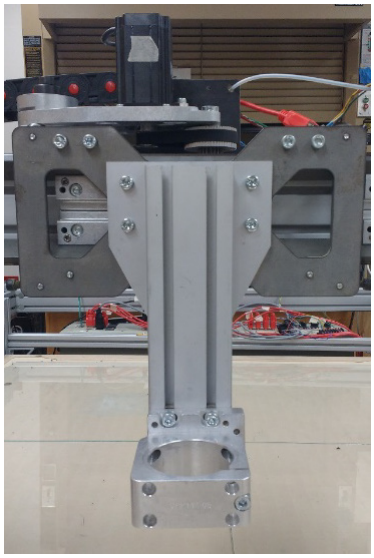

Figure 3.5. Tool holder.

Figure 3.6. Z axis mechanism.

Figure 3.7. Acme nut.

Four 5 start Acme lead screw is attached to each corner of the machine frame with bearings and coupled to stepper motors which are mounted on the bottom of the frame (Figure 3.6). The printer bed is attached to the four lead screw using an Acme nut (Figure 3.7), translating rotational motion of the screw into linear motion. The bed itself was constructed from 4080 T-slot aluminum extrusion to be the shape of rectangle, with medium density fiberboard (MDF) fixed on top of the bed. To ensure smooth surface for 3-D printing, eight 23” x 23” rectangular glass was placed on top of the bed and fixed in place to prevent movement during 3-D printing process.

The X and Y axis motion mechanism is based on rack and pinion system. A pulley is attached to the shaft of the stepper motor, driving roller drive spindle with a timing belt

(Figure 3.8). A gear rack is attached along the linear rail for X and Y axis, engaging the roller drive spindle and translates rotational motion of the roller drive spindle into linear motion. The roller drive spindle is pressed against the gear rack using a spring tension system.

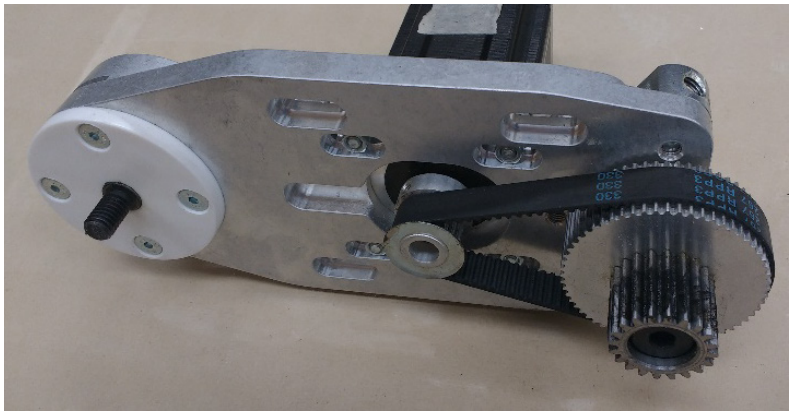

Figure 3.8. Rack and Pinion Drive.

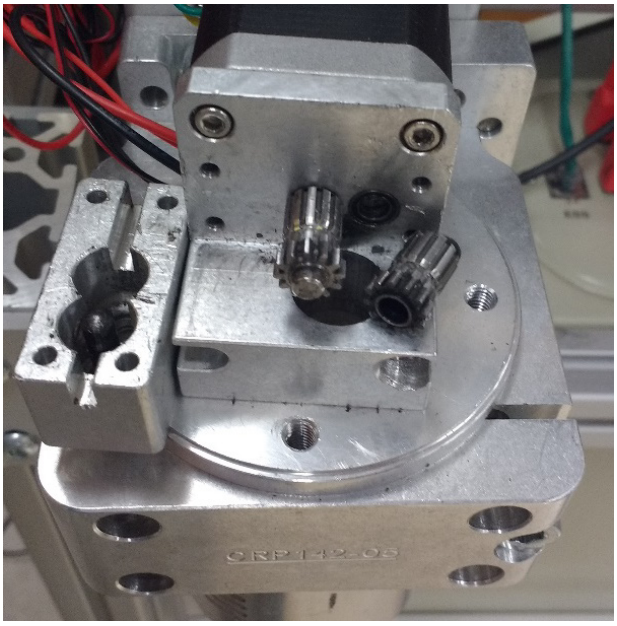

Figure 3.9. Extruder.

The last part of the mechanical system is the extruder drive for pushing plastic filament out of the nozzle in the FFF process. An assembly of motor, extruder, hot end holder and hot end is mounted on the tool holder. A direct drive extruder is designed and machined by CNCRouterParts for mounting directly on the tool holder. A direct drive extruder is preferred instead of a Bowden extruder because the gantry is already carrying heavy aluminum extrusion and metal tool holder, which eliminates the advantage of a Bowden extruder. The motor mount is designed to fit NEMA 17 motor, driving a pair of drive gear that pinch the filament and push it to the hot end holder. The design of the extruder does not have a spring tension mechanism for pinching the filament, so the drive gear could grind the filament. For this reason, the current settings of the extruder stepper driver must be set accordingly to limit the torque of the extruder motor.

A hot end holder is custom machined to be able to hold a variety of common hot end (Figure 3.10). Each hot end might have different length and might not fill all the space inside the hot end holder, so a filler is designed and 3-D printed to fill the gap in the hot end holder (Figure 3.11). A bowden tube can be inserted inside the hot end filler to minimize friction. Any hot end with the top cylinder diameter of around 15 mm will work for the hot end holder, but a Volcano hot end is chosen [122] because it has a larger heating element, which is required for high extrusion rates needed for printing large print volumes in reasonable amount of time. There will be more surface area contact between the filament and heating element to make sure the filament is properly heated before going out through the nozzle.

Figure 3.10. Hot end holder.

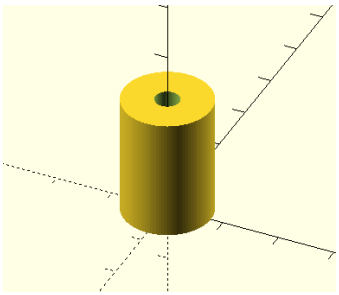

Figure 3.11. Hot end holder fill.

3.2.2 Electrical Design

The electrical system of the existing CNC machine consists of a sensors subassembly, motor subassembly, and main controller. The sensor subassembly consists of inductive sensors as limit switch (Figure 3.12), hot end temperature sensor, and sensor interface circuit board (Figure 3.13). The inductive sensor used has self-contained electronics with NPN output. It has 8 mm detection distance for steel which is required for these types of machines so that the heavy load carried by the stepper motor has time to stop before smashing into the sensor.

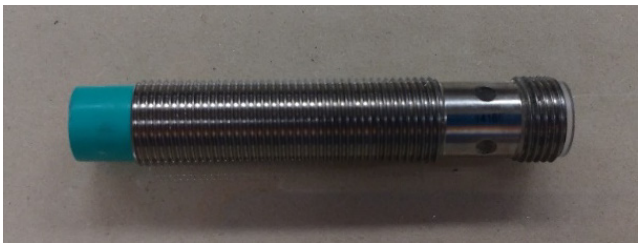

Figure 3.12. Inductive sensor.

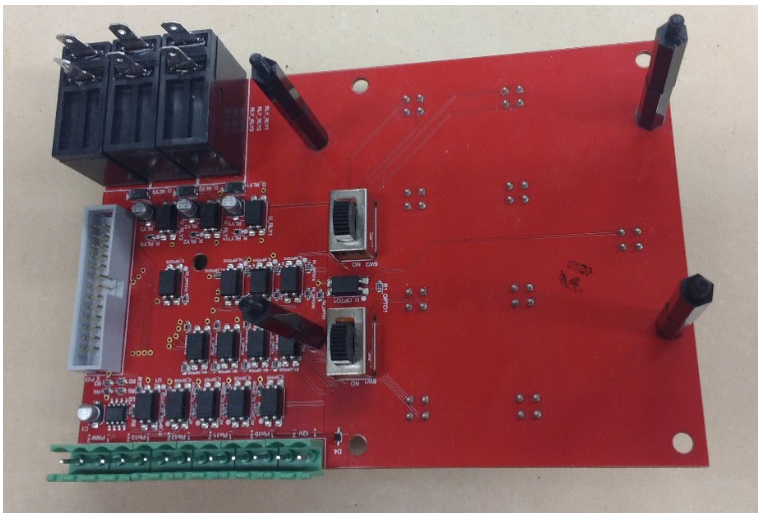

Figure 3.13. Sensor interface board.

Seven inductive sensors were used in total, one for minimum Y axis, two for minimum X axis, and four for maximum Z axis. The sensor interface board provide optocouplers to decouple the signal from the inductive sensors to the controller board. The signal from the temperature sensor of hot end, usually analog voltage from thermistor, is connected directly to the analog to digital converter of the custom made main interface board.

The motor subassembly consists of stepper motors, stepper driver (Figure 3.14), and motor interface circuit board (Figure 3.15). Seven NEMA 23 stepper motors were used for the motion system, one for Y axis, two for X axis and four for Z axis. One NEMA 17 stepper motor is used for the extruder. Multiple standalone stepper driver CRP5042 are used to drive each stepper motors with selectable output current and microstep resolution. The motor interface board is used to route the stepper driver signal to the controller board. The board does not have any electronics because the stepper driver already has built in optocoupler.

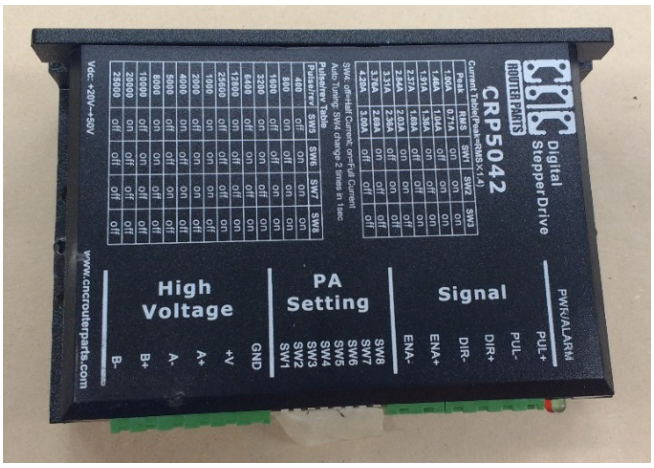

Figure 3.14. Stepper driver.

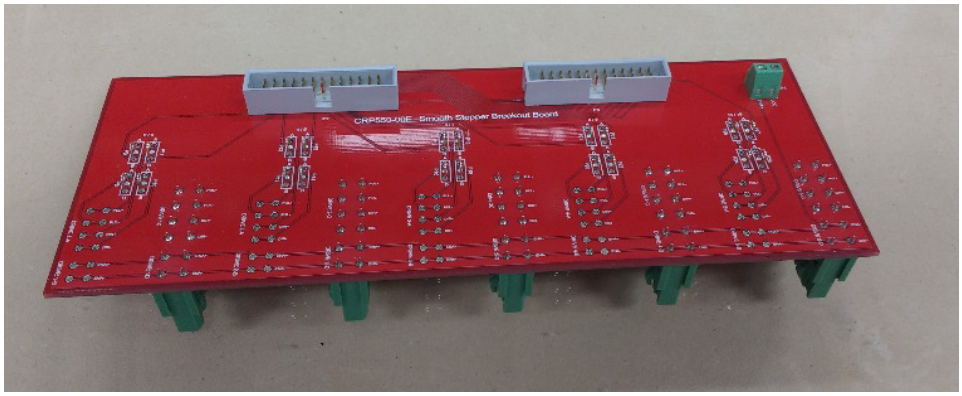

Figure 3.15. Motor interface board.

The controller board used for running the 3-D printer controller is beaglebone green [123]. As the software controller needs another microcontroller board to host the firmware, a microcontroller board was custom designed using KiCad containing ATmega1284p with its supporting circuit, logic buffer chip for providing current needed to drive optocoupler inside the stepper driver, level shifting chip for translating 5 V logic of ATmega to the 3.3 V logic of beaglebone, and power transistors for driving hot end and fan. Any equivalent open source 3-D printer controller board could also be used as the interface between beaglebone and the existing electronics system.

3.2.3 Software

There are many open source 3-D printer controllers available, but few software programs have the capability to handle 8 stepper motors and 7 limit switches that this machine have. The software must also be able to synchronize the four motors of Z axis and two motors of X axis so that they could move together at the same time. Another concern is the ability to extend the functionality of the machine by changing the tool head.

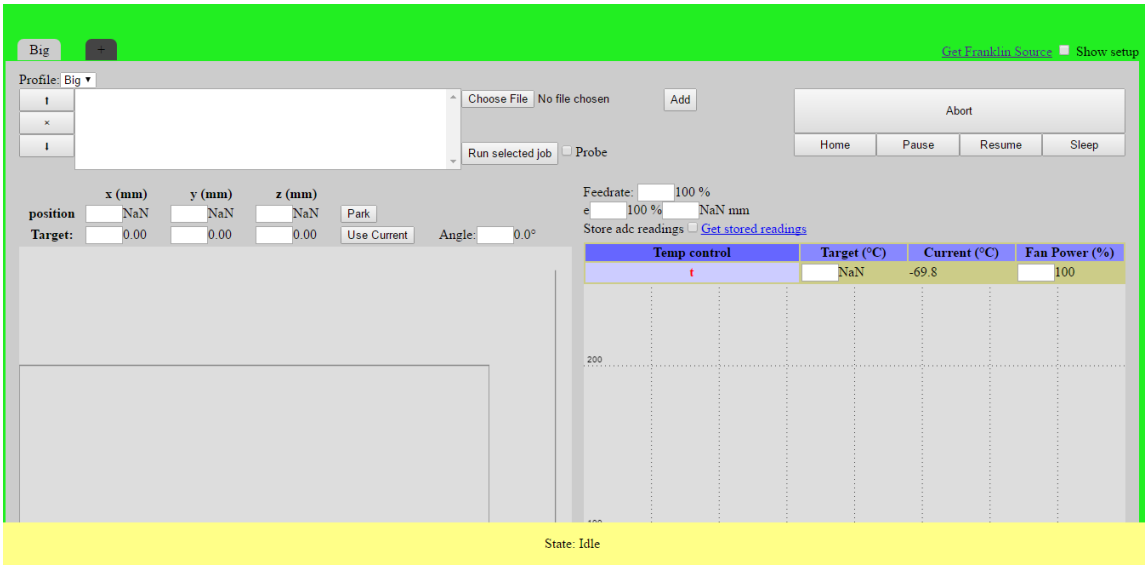

Figure 3.16. Franklin web interface [124].

For those reasons, Franklin [124], [125], a free and open source 3-D printer controller that runs on the open source Debian operating system [126], is chosen. The user interface for Franklin is a web interface accessed with a web browser (Figure 3.16). Franklin has a feature called follower motor, which configures a motor to follow another motor. This feature enables the operation of multiple motors on one axis, such as the one on this machine. This software also enables easy calibration, by adding an offset value to each motor. This feature can be used for X axis and Z axis calibration by adding an offset to one or several motors in the axis.

The motor and sensor configuration for Franklin can be changed easily in the web interface. Each pin on the microcontroller interface board can be set to function as output to stepper driver or input from sensor interface board. The logic could also be set active high or low. Franklin functionality can be extended by writing python script, utilizing existing python library to control printer operation. Experienced users can also modify the code and add additional features as there are some resources that will help to understand Franklin's internal working structure.

3.3 Quality Control

3.3.1 Safety

Unlike desktop 3-D printers this machine is an industrial machine that poses mechanical hazards to operators. To ensure the safety, there is several emergency stop switches provided with the existing CNC kit. They could function as hard stop switch, cutting of electrical signal to the motor directly by driving the enable pin of stepper driver and software stop switch, which would signal the software Franklin to stop operating the machine. There are several hard stop switches on the side of electrical panel box containing the electronic circuitry and one software stop switch on the opposite side of the machine (Figure 3.17).

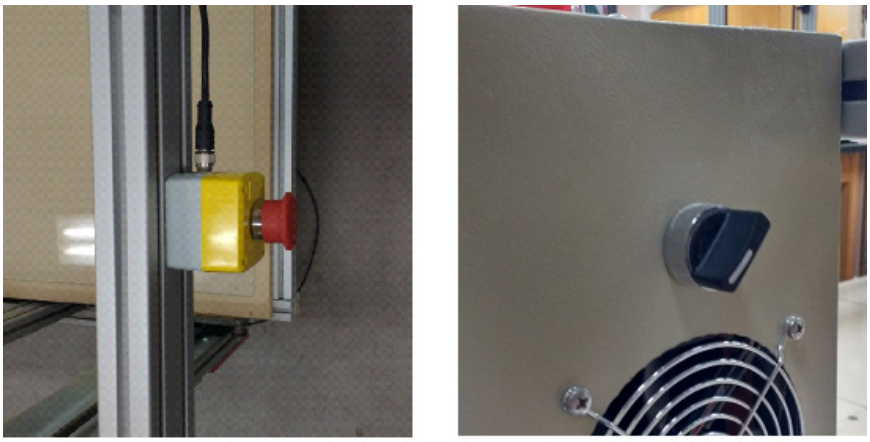

Figure 3.17. Emergency switch (a) software emergency switch (b) hard emergency switch.

The original CNC machine had the bed fixed and does not have Acme lead screw on the inside of the frame. The holder for the screw could block the movement of the printer head near the minimum and maximum y axis. For this reason, a sensor holder is designed and 3-D printed that moved the position of Y inductive limit switch (Figure 3.18).

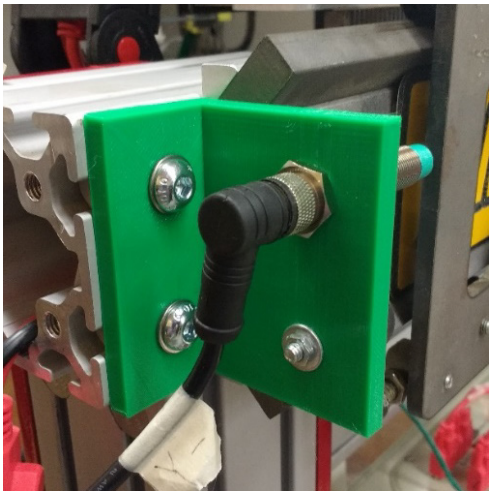

Figure 3.18. 3-D printed sensor holder.

When printing large size 3-D model, the bed adhesion might be too strong when removing the finished object. The glass on the surface of the bed might break when trying

to remove big prints. Using kapton tape or blue painter tape on top of the glass surface will help during the print removal process.

Extra stress on the nozzle during printing process is also a potential problem. The mechanical motion system of the machine is stronger than desktop 3-D printer and might break fragile part of the hot end. Over extrusion or a lot of overhangs on the print might introduce bumps on the top layer of the printed object that could collide with the nozzle head. A hot end cover will protect the hot end during the printing process.

3.3.2 Calibration

Calibration is very important for a 3-D printer as it directly affects the quality of the print results. The frame is already rigid such that there is no significant variations along each dimensions. In spite of that, some calibration is still needed to ensure that each axis is perpendicular to each other, the movement of each axis is precise down to sub-mm, and the bed is level relative to the nozzle of the printer head.

X axis

The X axis needs to be calibrated since the relative position between the two X axis motors will determine whether X and Y axis are perpendicular or not. If the frame is properly built, the rubber bumpers attached to the edge of X axis (Figure 3.19) will be aligned such that they are perpendicular to the X axis. So the initial calibration can be done during the built process by moving the gantry to the minimum X axis until both of its leg are touching the bumpers. After that adjust both the inductive switches to touch both legs to calibrate the switches position. Verifying if both axes are perpendicular can be done by printing a big square and measuring the angle of the corner of the square. Additional calibration can be done in software by adding offset value to one of the motors. The amount of offset needed can be calculated from measuring the printed square angle.

Figure 3.19. Bumpers.

Z axis

Four inductive limit switches were fixed at the bottom of the frame near the four motors that serves as the maximum limit for each Z motor. This configuration is chosen because if the limit switches were to be installed at the top as the minimum limit, then the position of each limit switches has to be exactly the same height with the nozzle of the printer. Setting the limit switches as the maximum limit enables the zero Z coordinate for each motor to be set in software.

Initial calibration can be done by moving the bed to the bottom of the bed until it touches the frame of the machine. After that, using the existing CNC spindle head, carve out an indentation on the MDF to put the glass as the surface of the bed. Software calibration can be done by moving the printer nozzle to each corner of the bed, then slowly raise the bed to touch the nozzle and put a piece of paper between the nozzle and the glass bed. The nozzle and the bed should pinch the paper so that it is still possible to move but some drag is felt. The offset value of each Z motor should be changed until different corner of the bed is level.

Due to the bed of the machine made of MDF, over time it might absorb moisture and deformed. This results in the bed not being level at all points down to sub-mm and some points might have poor bed adhesion. Using brim or raft will help with the bed adhesion. Printing a thicker first layer and calibrating the bed to match the lowest point on the bed will also help.

Determining Steps per mm

Figure 3.20. Roller drive spindle.

The X and Y axis used rack and pinion system to translate rotational movement of the stepper motor into linear motion. The motor shaft is attached to a 22 tooth pulley with 1" pitch circle diameter. The pulley is attached to the roller drive spindle (Figure 3.20) with a timing belt. The roller drive spindle has 60:22 gear ratio so the distance traveled per motor revolution is

$$\mathrm{D} = \frac{N_A}{N_B} * \pi * PCD_A \qquad (2)$$

with D is the linear distance traveled in inch, N_A and N_B respectively are number of teeth of pulley and roller drive spindle and PCD_A is the pitch circle diameter of the pulley. Then steps/mm is

$$\text{Steps/mm} = \frac{PPR}{D\ (in\ mm)} \tag{3}$$

with PPR is pulse per revolution, could be configured on the stepper driver. At 2000 PPR, the steps/mm for X and Y axis is 68.356.

Z axis uses a 5 start Acme lead screw that coupled directly with the shaft of the Z motors. The distance traveled per motor revolution is

$$\text{D} = \frac{Starts}{TPI} \tag{4}$$

with D is the linear distance traveled in inch, Starts is the number of starts or how many threads on the screw, TPI is the threads per inch. Then steps/mm is calculated the same way as in (3). The lead screw has 10 threads/inch. At 2000 PPR, the steps/mm for Z axis is 157.48.

For the extruder, the distance traveled per motor revolution is simply the effective circumference of the drive gear. The steps/mm is calculated the same way as in (3). The drive gear has around 9 mm effective diameter, so it has effective circumference of 9π mm. At 2000 PPR, steps/mm will be 70.736.

3.3.3 General Testing

There are a few hardware and software testing that could help to ensure proper operation of the machine. Before operating the machine for the first time, the direction of the movement of each stepper motor and the function of the limit switches are verified to prevent the machine crashing into the limit switches. Each axis was moved manually in software and they should stop before hitting the limit switches. The LED indicator on the inductive limit switch will lit when a metal is detected in front of it, indicating that the sensor is working correctly. The movement of each axis was also tested to ensure they can move accurately along all dimension within the defined limits. The test was done by manually moving each axis to several points back and forth and checking if the point where they stop matches the coordinate shown in the software. Improper assembly of the mechanical motion systems or wrong steps/mm might be some of the reasons why this test could fail. The correct current settings for each motor must also be configured so that the motor has enough torque to move the axis without overheating the motor.

The extruder was also tested to ensure they can extrude the intended filament accurately. The actual length of the filament going into the extruder is measured and then compared with the extruded length shown in software. The actual steps/mm will then become

$$\text{Steps/mm (actual)} = \frac{L1}{L2} * Steps/mm\ (current) \tag{5}$$

where L1 is the extruded length shown in software and L2 is the actual length going into the extruder. The actual temperature on the hot end is also measured and compared with the temperature shown in software. If they does not match, wrong thermistor value is inserted or the thermistor might be broken. The final test on the extruder is to ensure that it can extrude and retract the filament currently being used. Different filament have different strength and stiffness, so the extruder might require different extrusion and retraction settings as discussed in [127]. The current for extruder motor must also be configured so it has enough torque to push the filament, but not too much that it starts grinding the filament.

3.4 Application

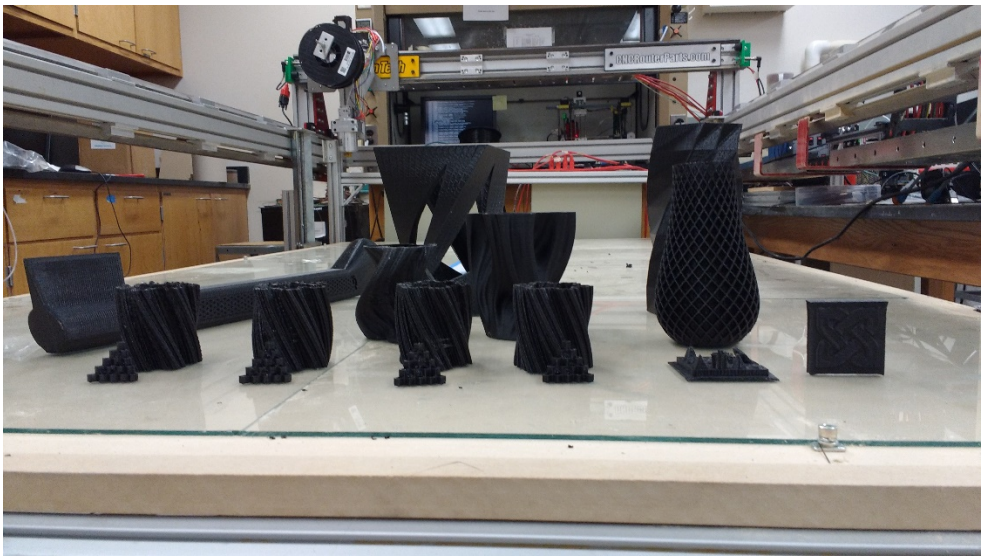

Figure 3.21. The 3-D printer with its printed objects.

The finished system can be seen in Figure 3.21. The machine has been used to print test objects that showed the capability of the printer to print small detailed object to medium sized object. Generally, FFF 3-D printer technology have adjustable parameter that trade quality for speed. The printed objects showcased here are optimized for quality. Printing bigger object, which is the intended application of this machine, will be optimized for speed which will make the printed quality not as good as showcased here.

3.4.1 Printed Parts

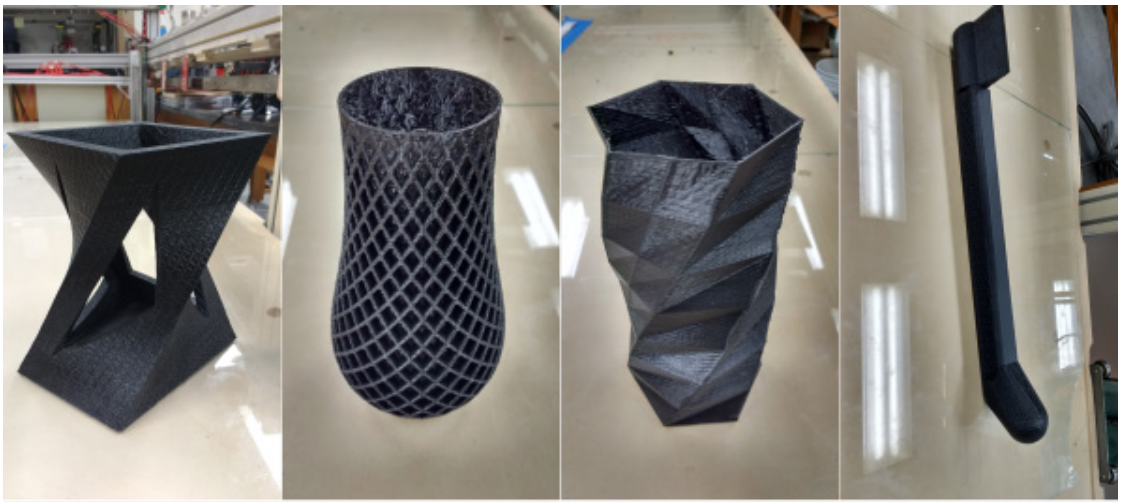

(a) (b) (c) (d)

Figure 3.22. Printed 3-D object (a) Box vase (3D design source from [128]) (b) Spiral vase (3D design source from [129]) (c) Twisted 6-sided vase (3D design source from [130]) (d) Axe handle.

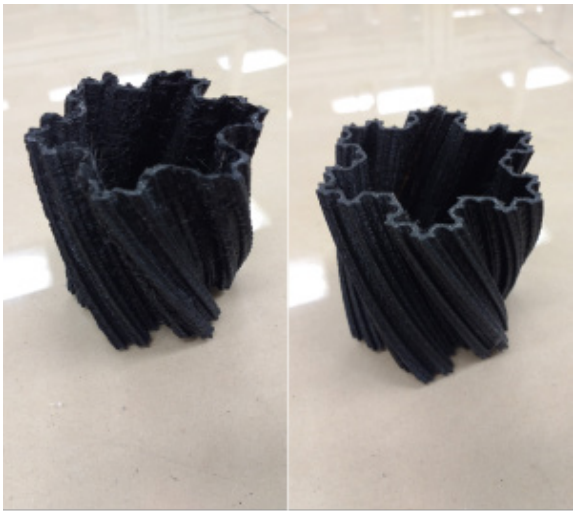

(a) (b)

Figure 3.23. Koch snowflake vase (3D design source from [131]) printed with speed (a) 100 mm/s (b) 25 mm/s.

Figure 3.22 showed a variety of object printed with the machine. Figure 3.22 (a) is a Box vase printed with 0.5 mm nozzle, 0.2 mm layer height, and 70 mm/s speed. It took

about 17 hours to print 15 x 15 x 15 cm model with 25 % infill. Figure 3.22 (b), (c) and (d) used almost the same print parameter with slower speed of around 50 mm/s to achieve good quality result. Figure 3.23 showed a comparison of difference in quality for complex features when the print speed is varied. Both are printed with 0.5 mm nozzle and 0.2 mm layer height, but the speed of Figure 3.23 (a) is four times faster than Figure 3.23 (b). It can be seen that Figure 3.23 (b) have sharper edges and resemble snowflake better.

3.4.2 Reuse Potential and Adaptability

The machine was designed to fill the void in an open source large form factor 3-D printer. As such, the software controller was selected with easy extendable function in mind. The target audience is researchers and engineers with skills in mechanical engineering, electrical engineering, and 3-D printing technology. With the design files easily accessible, anyone is able to optimize and tailor the machine for their own needs.

The hardware could be reused in many applications such as:

1. The design is modular such that the mechanical system, electrical system, or the software could be reused. For example, the mechanical motion could be used for another application requiring linear motion. Franklin can be used for any purpose with the addition of a python script.
2. The tool head could be changed easily and controlled with the python script. This would enable the entire platform itself to be used as an automated scientific tool [132] (e.g. for combinatorial fluid handling).
3. Adding another axis to create multi axis additive or subtractive manufacturing following what has been done with smaller RepRap style machines [118].

Extending the functionality of the machine or using different component to substitute the current component requires some understanding of the mechanical or electrical system. There are several support mechanism available. For Franklin, users can post questions on the MOST delta users forum [133]. For mechanical design, there are

many support forums for CNC machine enthusiasts and also build instructions and documentations from CNCRouterParts. The electrical system is mostly from CNCRouterParts with the addition of interface board and beaglebone green. Readers could contact the authors for support about this addition or see a how-to page from [134]. Alternatively, equivalent open source 3-D printer controller or microcontroller board could also be used as the interface board. There are also a lot of support forums regarding these open source electronics.

3.5 Build Details

3.5.1 Availability of Materials and Methods

All mechanical and almost all electrical parts were from CNCRouterParts and can be ordered from their website directly. The rest of the electronics is just the interface board, a single board computer beaglebone green, and a hot end. Information for the interface board is given in [134]. The hot end used is a standard volcano hot end which is available in many 3-D printing vendors. Software Franklin is open source and can be downloaded from github [124]. There are several image file readily available for installing Franklin and Debian operating system on beaglebone green using microsd card.

3.5.2 Ease of Build

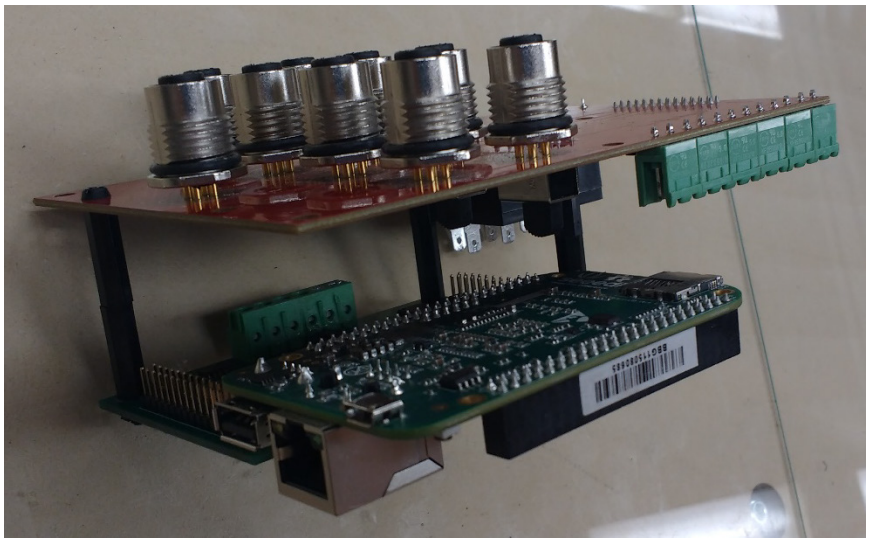

Figure 3.24. Assembly of interface boards and beaglebone green.

The existing CNC machine from CNCRouterParts have been designed to be easily assembled by average-skilled users. There is video and instructions at their website [135] for building the machine. Most of the electronics is also on their website and are ready to use. The custom interface board is designed to easily plug into beaglebone green using header female and male pair (Figure 3.24). The interface board is also designed to be tightened to the sensor interface board using spacers for easy assembly and placement. The pinout of main interface board was also designed to connect to the existing sensor and motor interface board easily using a ribbon cable (Figure 3.25).

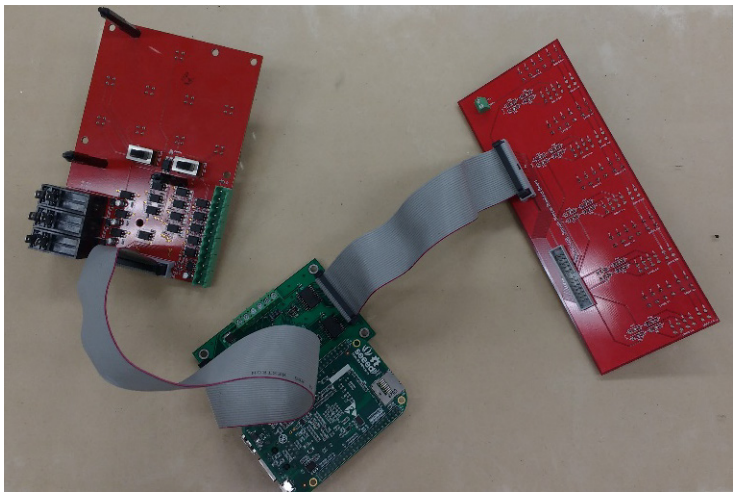

Figure 3.25. Ribbon cable connection between several circuit boards.

There are some settings in Franklin that needs to be changed to use the interface board. An instruction page for using Franklin for CNCRouterParts machine is available at [136]. A configuration file for Franklin is also provided so that given the wiring configuration provided in the instructions, the user could just import the file and start using the machine instead of configuring them manually.

3.5.3 Operating Software and Peripherals

Franklin is an open source 3-D printer controller developed in C++ and python. It runs on Debian operating system and could be accessed remotely using web interface. Any hardware that could run Debian would be a suitable platform for Franklin. Franklin needs at least four GPIO for flashing firmware into the microcontroller board and one serial interface for communicating to the firmware. The software consists of a server, python

driver, C driver, and firmware. The firmware of Franklin is designed for AVR architecture and uses several assembly instructions for critical parts of the firmware. For this machine, the firmware needs a microcontroller that has 26 GPIO (16 for stepper driver, 7 for inductive limit switch, 1 for hot end, 1 for fan, 1 for emergency stop) and 1 ADC for thermistor reading. It was tested to work on ATmega1284p but could also be used for many other equivalent open source 3-D printer electronics.

Cura version 15.04.6 was tested to slice 3-D models into gcode file that works with Franklin. Franklin does not support some gcode so there needs to be specific start and end gcode for Cura which could be found at [137] to ensure proper operation of Franklin.

3.6 Discussion

3.6.1 Conclusions

Development of open source hardware could accelerate innovation and improve design quality. This project demonstrates that open source components could be used to accelerate development. This project alone will not be possible without the availability of modular components such as CNC machine from CNCRouterParts, Beaglebone green, Arduino, Franklin, Debian, and Debian Linux software development tools to build the firmware and software from. The availability of documentation and specification from CNCRouterParts, especially the electronic parts is also indispensable to this project, as it enables the use of existing electrical and electronic system and requires only the addition of an interface board and beagle bone green. The availability and support from Franklin also helps bring the machine to reality.

Lesson learned from design iterations include an appreciation for the availability of documentation. Without it, it would be hard to interface with the existing electrical and electronic system and the developer would have to resort to trial and error, which significantly increases development time.

3.6.2 Future Work

This system can be improved by pushing it further down the path of free and open source hardware design. This would include open sourcing the patented linear guide device from CNCRouterParts [121]. In addition, there are also several attempts in literature to extend functionality of a CNC Machine with additive manufacturing capability such as [138]. The difference is they used gas metal arc welding instead and create a hybrid additive-subtractive machine. Using the machine as hybrid manufacturing would be easier with magnetically mounted tool heads following [118]. Big size FFF 3-D printers usually would need bigger nozzle so that the printing time does not take too long. Therefore there is also a need to custom design hot end with bigger nozzle. Currently the filament available on the market is only in 1.75 mm and 3 mm, so to use bigger nozzle a pellet extruder needs to be used. There are relevant papers describing the physics behind it [139], [140], and several open source projects [141], [142].

Alternative open source 3-D printer microcontroller board such as RAMPS [143] could also be used as the interface board with some addition, increasing versatility of the system. It would also be interesting to evaluate the ability of this system to support a small-distributed manufacturing business [144].

Chapter 4
Conclusion

4.1 Conclusions

Two applications of the open source 3-D printer platform have been investigated. Both projects have used some parts from the 3-D printer platform community to speed up the development of the equipment. The first project completely reused the 3-D printer and its software as a precise positioning platform. In the spirit of open source hardware, it was deemed possible to cut down the costs even more by designing in-house current source circuit, voltage measurement circuit, and Java user interface. The resulting measurement circuit, showed promising results. The measurement results, provided it is used for ITO or similar material, was comparable to some of the commercial equipment at Michigan Tech. Moreover, we can completely automate the measurement by writing a script in Java to perform multiple measurement on different points on the sample.

The second project utilizes the FFF extrusion process knowledge and parts from 3-D printing community and also an open source 3-D printer controller developed at Michigan Tech. Any precise mechanical motion system, such as the one on CNC machine, could be retrofitted to be a FFF 3-D printer. The resulting machine, with proper use by FFF technology experts, is able to print some simple and complex 3-D object with comparable quality to most desktop 3-D printer.

The conclusion of this investigation is that it is possible to reuse some parts of the open source 3-D printer platform to accelerate development of research and manufacturing equipment, with the resulting equipment comparable in quality to commercial equipment.

The RepRap project is still evolving and has the potential to be reused in many other applications in the future. In analogy with open source software such as Linux, the initial stages of many open source projects were not intended to be used by novice users. It is targeted toward makers, developers and researchers who know the technology they are working on, can fix any problems that occurs and contribute to the project. As the RepRap project evolves, it will become more mature and become more user friendly and stable. Just like any other open source software, open source hardware have the potential to accelerate innovation, provide better quality hardware in the long run provided there is enough contributor, and reduce the cost of hardware.

4.2 Future Work

Open Source Automated Mapping Four-Point Probe

1. Using more accurate, standalone Analog to Digital Converter (ADC) instead of the built in ADC on board the microcontroller would improve the measurement performance
2. Design current source circuit with higher compliance voltage and higher current output, so that the circuit could measure material with higher and lower resistance and contact resistance.
3. Add sample protection circuit to protect the sample from high voltages and current
4. Design another measurement circuit topology that does not suffer from imprecise value and matching of the resistors, finite ON state resistance of reed relays, current leakage due to op-amp.
5. Prevent the saturation of instrumentation amplifier
6. Include correction factor calculator in the Java software
7. Provide better error message and information about the measurement process
8. Improve the detection of whether there are sample or not

9. Use a pellet extruder instead of filament extruder for lower cost of printing materials and allowing the use of a bigger nozzle
10. Automatic bed levelling using inductive sensor and python script extension
11. Find better bed materials because the current MDF is sensitive to moisture and the glass bed is prone to breaking when removing big prints
12. Enclosed build chamber for better print quality and enabling the use of more material without warping problem
13. Multiple gantry and print head for faster printing and printing multiple copies at once
14. Hybrid additive and subtractive manufacturing. The subtractive manufacturing could provide better finish and accurate dimensioning than additive manufacturing
15. A filament direct extruder that have adjustable pinch pressure to allow more grip for soft, slippery and rubbery materials.

REFERENCES

[1] M. Woelfle, P. Olliaro, and M. H. Todd, "Open science is a research accelerator," *Nat Chem*, vol. 3, no. 10, pp. 745–748, Oct. 2011.

[2] A. Hansen and T. J. Howard, "The Current State of Open Source Hardware: The Need for an Open Source Development Platform," in *ICoRD'13*, A. Chakrabarti and R. V. Prakash, Eds. Springer India, 2013, pp. 977–988.

[3] R. Jones *et al.*, "RepRap – the replicating rapid prototyper," *Robotica*, vol. 29, no. 1, pp. 177–191, Jan. 2011.

[4] C. Baechler, M. DeVuono, and J. M. Pearce, "Distributed recycling of waste polymer into RepRap feedstock," *Rapid Prototyping Journal*, vol. 19, no. 2, pp. 118–125, Mar. 2013.

[5] S. Chong, G.-T. Pan, M. Khalid, T. C.-K. Yang, S.-T. Hung, and C.-M. Huang, "Physical Characterization and Pre-assessment of Recycled High-Density Polyethylene as 3D Printing Material," *J Polym Environ*, pp. 1–10, Jul. 2016.

[6] J. M. Pearce, "Building Research Equipment with Free, Open-Source Hardware," *Science*, vol. 337, no. 6100, pp. 1303–1304, Sep. 2012.

[7] J. M. Pearce, *Open-Source Lab: How to Build Your Own Hardware and Reduce Research Costs*, 1st ed. Amsterdam: Elsevier Science Publishers B. V., 2013.

[8] T. Baden, A. M. Chagas, G. Gage, T. Marzullo, L. L. Prieto-Godino, and T. Euler, "Open Labware: 3-D Printing Your Own Lab Equipment," *PLOS Biol*, vol. 13, no. 3, p. e1002086, Mar. 2015.

[9] B. Wijnen, G. C. Anzalone, and J. M. Pearce, "Open-source mobile water quality testing platform," *Journal of Water Sanitation and Hygiene for Development*, vol. 4, no. 3, pp. 532–537, Sep. 2014.

[10] C. D. Kelley *et al.*, "An Affordable Open-Source Turbidimeter," *Sensors*, vol. 14, no. 4, pp. 7142–7155, Apr. 2014.

[11] D. M. Laverty, R. J. Best, P. Brogan, I. A. Khatib, L. Vanfretti, and D. J. Morrow, "The OpenPMU Platform for Open-Source Phasor Measurements," *IEEE Transactions on Instrumentation and Measurement*, vol. 62, no. 4, pp. 701–709, Apr. 2013.

[12] C. Zhang, N. C. Anzalone, R. P. Faria, and J. M. Pearce, "Open-Source 3D-Printable Optics Equipment," *PLOS ONE*, vol. 8, no. 3, p. e59840, Mar. 2013.

[13] M. C. Carvalho and B. D. Eyre, "A low cost, easy to build, portable, and universal autosampler for liquids," *Methods in Oceanography*, vol. 8, pp. 23–32, Dec. 2013.

[14] G. Niezen, P. Eslambolchilar, and H. Thimbleby, "Open-source hardware for medical devices," *BMJ Innov*, vol. 2, no. 2, pp. 78–83, Apr. 2016.

[15] E. T. da Costa, M. F. Mora, P. A. Willis, C. L. do Lago, H. Jiao, and C. D. Garcia, "Getting started with open-hardware: development and control of microfluidic devices," *Electrophoresis*, vol. 35, no. 16, pp. 2370–2377, Aug. 2014.

[16] T. H. Lücking, F. Sambale, B. Schnaars, D. Bulnes-Abundis, S. Beutel, and T. Scheper, "3D-printed individual labware in biosciences by rapid prototyping: In vitro biocompatibility and applications for eukaryotic cell cultures," *Eng. Life Sci.*, vol. 15, no. 1, pp. 57–64, Jan. 2015.

[17] B. C. Gross, J. L. Erkal, S. Y. Lockwood, C. Chen, and D. M. Spence, "Evaluation of 3D printing and its potential impact on biotechnology and the chemical sciences," *Anal. Chem.*, vol. 86, no. 7, pp. 3240–3253, Apr. 2014.

[18] C.-K. Su, S.-C. Hsia, and Y.-C. Sun, "Three-dimensional printed sample load/inject valves enabling online monitoring of extracellular calcium and zinc ions in living rat brains," *Anal. Chim. Acta*, vol. 838, pp. 58–63, Aug. 2014.

[19] M. Maldonado-Torres, J. F. López-Hernández, P. Jiménez-Sandoval, and R. Winkler, "'Plug and Play' assembly of a low-temperature plasma ionization mass spectrometry imaging (LTP-MSI) system," *J Proteomics*, vol. 102, pp. 60–65, May 2014.

[20] J. N. Wittbrodt, U. Liebel, and J. Gehrig, "Generation of orientation tools for automated zebrafish screening assays using desktop 3D printing," *BMC Biotechnology*, vol. 14, p. 36, 2014.

[21] T. R. Damase, D. Stephens, A. Spencer, and P. B. Allen, "Open source and DIY hardware for DNA nanotechnology labs," *Journal of Biological Methods*, vol. 2, no. 3, p. e24, Aug. 2015.

[22] K.-H. Herrmann, C. Gärtner, D. Güllmar, M. Krämer, and J. R. Reichenbach, "3D printing of MRI compatible components: why every MRI research group should have a low-budget 3D printer," *Med Eng Phys*, vol. 36, no. 10, pp. 1373–1380, Oct. 2014.

[23] J. M. Pearce, "Laboratory equipment: Cut costs with open-source hardware," *Nature*, vol. 505, no. 7485, pp. 618–618, Jan. 2014.

[24] J. M. Pearce, "Quantifying the Value of Open Source Hard-ware Development," *Modern Economy*, vol. 06, no. 01, pp. 1–11, 2015.

[25] J. M. Pearce, "Return on investment for open source scientific hardware development," *Science and Public Policy*, p. scv034, Jun. 2015.

[26] C. Zhang, B. Wijnen, and J. M. Pearce, "Open-Source 3-D Platform for Low-Cost Scientific Instrument Ecosystem," *Journal of Laboratory Automation*, vol. 21, no. 4, pp. 517–525, Aug. 2016.

[27] B. Wijnen, E. E. Petersen, E. J. Hunt, and J. M. Pearce, "Free and open-source automated 3-D microscope," *J Microsc*, Aug. 2016.

[28] J. Kurz, "Apricum's Global PV's 5 year outlook - strong continued growth," *Apricum - The Cleantech Advisory*, 03-Aug-2015.

[29] "The 2016 Global PV Outlook: US, Asian Markets Strengthened by Policies to Reduce CO2." [Online]. Available: http://www.renewableenergyworld.com/articles/2016/01/the-2016-global-pv-outlook-u-s-and-asian-markets-strengthened-by-policies-to-reduce-co2.html. [Accessed: 29-Aug-2016].

[30] J. M. Pearce, "Photovoltaics — a path to sustainable futures," *Futures*, vol. 34, no. 7, pp. 663–674, Sep. 2002.

[31] K. Branker, M. J. M. Pathak, and J. M. Pearce, "A review of solar photovoltaic levelized cost of electricity," *Renewable and Sustainable Energy Reviews*, vol. 15, no. 9, pp. 4470–4482, Dec. 2011.

[32] R. E. Smalley, “Future Global Energy Prosperity: The Terawatt Challenge,” *MRS Bulletin*, vol. 30, no. 6, pp. 412–417, Jun. 2005.

[33] A. Vora, J. Gwamuri, N. Pala, A. Kulkarni, J. M. Pearce, and D. Ö. Güney, “Exchanging Ohmic losses in metamaterial absorbers with useful optical absorption for photovoltaics,” *Sci Rep*, vol. 4, p. 4901, 2014.

[34] A. Vora, J. Gwamuri, J. M. Pearce, P. L. Bergstrom, and D. Ö. Güney, “Multi-resonant silver nano-disk patterned thin film hydrogenated amorphous silicon solar cells for Staebler-Wronski effect compensation,” *Journal of Applied Physics*, vol. 116, no. 9, p. 093103, Sep. 2014.

[35] A. Tamang, H. Sai, V. Jovanov, S. I. H. Bali, K. Matsubara, and D. Knipp, “On the interplay of interface morphology and microstructure of high-efficiency microcrystalline silicon solar cells,” *Solar Energy Materials and Solar Cells*, vol. 151, pp. 81–88, Jul. 2016.

[36] C. Onwudinanti, R. Vismara, O. Isabella, L. Grenet, F. Emieux, and M. Zeman, “Advanced light management based on periodic textures for Cu(In,Ga)Se_2 thin-film solar cells,” *Opt Express*, vol. 24, no. 6, pp. A693-707, Mar. 2016.

[37] H. Tan *et al.*, “Highly Efficient Hybrid Polymer and Amorphous Silicon Multijunction Solar Cells with Effective Optical Management,” *Adv. Mater. Weinheim*, vol. 28, no. 11, pp. 2170–2177, Mar. 2016.

[38] C. Zhang, D. O. Guney, and J. M. Pearce, “Plasmonic enhancement of amorphous silicon solar photovoltaic cells with hexagonal silver arrays made with nanosphere lithography,” *Mater. Res. Express*, vol. 3, no. 10, p. 105034, 2016.

[39] G. Conibeer *et al.*, “Silicon nanostructures for third generation photovoltaic solar cells,” *Thin Solid Films*, vol. 511–512, pp. 654–662, Jul. 2006.

[40] J. Gwamuri *et al.*, “Limitations of ultra-thin transparent conducting oxides for integration into plasmonic-enhanced thin-film solar photovoltaic devices,” *Mater Renew Sustain Energy*, vol. 4, no. 3, p. 12, Jul. 2015.

[41] H. Hanaei, M. K. Assadi, and R. Saidur, “Highly efficient antireflective and self-cleaning coatings that incorporate carbon nanotubes (CNTs) into solar cells: A review,” *Renewable and Sustainable Energy Reviews*, vol. 59, pp. 620–635, Jun. 2016.

[42] H. Sun, "Recent Progress in Anti-Reflection Layer Fabrication for Solar Cells," *Journal of Nanoelectronics and Optoelectronics*, vol. 11, no. 3, pp. 257–264, Jun. 2016.

[43] A. Tomasi *et al.*, "Transparent Electrodes in Silicon Heterojunction Solar Cells: Influence on Contact Passivation," *IEEE Journal of Photovoltaics*, vol. 6, no. 1, pp. 17–27, Jan. 2016.

[44] J. Gwamuri, M. Marikkannan, J. Mayandi, P. K. Bowen, and J. M. Pearce, "Influence of Oxygen Concentration on the Performance of Ultra-Thin RF Magnetron Sputter Deposited Indium Tin Oxide Films as a Top Electrode for Photovoltaic Devices," *Materials*, vol. 9, no. 1, p. 63, Jan. 2016.

[45] J. Gwamuri, A. Vora, J. Mayandi, D. Ö. Güney, P. L. Bergstrom, and J. M. Pearce, "A new method of preparing highly conductive ultra-thin indium tin oxide for plasmonic-enhanced thin film solar photovoltaic devices," *Solar Energy Materials and Solar Cells*, vol. 149, pp. 250–257, May 2016.

[46] T. Duong *et al.*, "Semitransparent Perovskite Solar Cell With Sputtered Front and Rear Electrodes for a Four-Terminal Tandem," *IEEE Journal of Photovoltaics*, vol. 6, no. 3, pp. 679–687, May 2016.

[47] L. B. Valdes, "Resistivity Measurements on Germanium for Transistors," *Proceedings of the IRE*, vol. 42, no. 2, pp. 420–427, Feb. 1954.

[48] F. M. Smits, "Measurement of sheet resistivities with the four-point probe," *The Bell System Technical Journal*, vol. 37, no. 3, pp. 711–718, May 1958.

[49] F. Keywell and G. Dorosheski, "Measurement of the Sheet Resistivity of a Square Wafer with a Square Four Point Probe," *Review of Scientific Instruments*, vol. 31, no. 8, pp. 833–837, Aug. 1960.

[50] M. A. Logan, "An AC Bridge for Semiconductor Resistivity Measurements Using a Four-Point Probe," *Bell System Technical Journal*, vol. 40, no. 3, pp. 885–919, May 1961.

[51] D. E. Vaughan, "Four-probe resistivity measurements on small circular specimens," *Br. J. Appl. Phys.*, vol. 12, no. 8, p. 414, 1961.

[52] L. J. Swartzendruber, “Four-point probe measurement of non-uniformities in semiconductor sheet resistivity,” *Solid-State Electronics*, vol. 7, no. 6, pp. 413–422, Jun. 1964.

[53] S. Yoshimoto *et al.*, “Four-Point Probe Resistance Measurements Using PtIr-Coated Carbon Nanotube Tips,” *Nano Lett.*, vol. 7, no. 4, pp. 956–959, Apr. 2007.

[54] S. Thorsteinsson *et al.*, “Accurate microfour-point probe sheet resistance measurements on small samples,” *Review of Scientific Instruments*, vol. 80, no. 5, p. 053902, May 2009.

[55] R. Ekawita, E. Rahmawati, M. Abdullah, and K., “Four point probe method based on LOG112 and C8051F006 SoCs for resistivity measurement,” in *2009 International Conference on Instrumentation, Communications, Information Technology, and Biomedical Engineering (ICICI-BME)*, 2009, pp. 1–3.

[56] P. Haibin, D. Jianning, W. Xiaofei, and L. Boquan, “Design, implementation, and assessment of a high-precision and automation measurement system for thin film resistivity,” in *2010 International Conference on Mechanic Automation and Control Engineering (MACE)*, 2010, pp. 2235–2238.

[57] I. Miccoli, F. Edler, H. Pfnür, and C. Tegenkamp, “The 100th anniversary of the four-point probe technique: the role of probe geometries in isotropic and anisotropic systems,” *J. Phys.: Condens. Matter*, vol. 27, no. 22, p. 223201, 2015.

[58] E. J. Zimney, G. H. B. Dommett, R. S. Ruoff, and D. A. Dikin, “Correction factors for 4-probe electrical measurements with finite size electrodes and material anisotropy: a finite element study,” *Meas. Sci. Technol.*, vol. 18, no. 7, p. 2067, 2007.

[59] A. Uhlir, “The potentials of infinite systems of sources and numerical solutions of problems in semiconductor engineering,” *The Bell System Technical Journal*, vol. 34, no. 1, pp. 105–128, Jan. 1955.

[60] D. S. Perloff, “Four- Point Probe Correction Factors for Use in Measuring Large Diameter Doped Semiconductor Wafers,” *J. Electrochem. Soc.*, vol. 123, no. 11, pp. 1745-1750, Nov. 1976.

[61] M. Yamashita and M. Agu, “Geometrical Correction Factor for Semiconductor Resistivity Measurements by Four-Point Probe Method,” *Japanese Journal of Applied Physics*, vol. 23, no. Part 1, No. 11, pp. 1499–1504, Nov. 1984.

[62] R. Rymaszewski, “Empirical method of calibrating a 4-point microarray for measuring thin-film-sheet resistance,” *Electronics Letters*, vol. 3, no. 2, pp. 57–58, Feb. 1967.

[63] R. Rymaszewski, “Relationship between the correction factor of the four-point probe value and the selection of potential and current electrodes,” *J. Phys. E: Sci. Instrum.*, vol. 2, no. 2, p. 170, 1969.

[64] D. K. Schroder, *Semiconductor Material and Device Characterization*, 2 edition. New York: Wiley-Interscience, 1998.

[65] F. Algahtani, K. B. Thulasiram, N. M. Nasir, and A. S. Holland, “Four point probe geometry modified correction factor for determining resistivity,” 2013, p. 89235D.

[66] “Jandel four point probes.” [Online]. Available: http://www.jandel.co.uk/products/four-point-probes.html. [Accessed: 07-Sep-2016].

[67] “Determining the Best Choice of Probe Tip Specifications for a Given Material,” *Four Point Probes*, 16-May-2013. [Online]. Available: http://four-point-probes.com/determining-the-best-choice-of-probe-tip-specifications-for-a-given-material/. [Accessed: 07-Sep-2016].

[68] “Four Point Probe Tip Specifications & Applications Chart,” *Four Point Probes*, 16-May-2013. [Online]. Available: http://four-point-probes.com/four-point-probe-tip-specifications-applications-chart/. [Accessed: 07-Sep-2016].

[69] S. Hasegawa *et al.*, “Direct measurement of surface-state conductance by microscopic four-point probe method,” *J. Phys.: Condens. Matter*, vol. 14, no. 35, p. 8379, 2002.

[70] “ADA4522-2 Datasheet and Product Info | Analog Devices.” [Online]. Available: http://www.analog.com/en/products/amplifiers/operational-amplifiers/ada4522-2.html#product-overview. [Accessed: 07-Sep-2016].

[71] V. Wang and V. Kusuda, “Zero-drift amplifiers: Now easy to use in high precision circuits,” *ResearchGate*, pp. 44–47, Sep. 2015.

[72] “Difference Amplifier Forms Heart of Precision Current Source: Analog Dialogue: Analog Devices.” [Online]. Available:

http://www.analog.com/library/analogDialogue/archives/43-09/current_source.html. [Accessed: 07-Sep-2016].

[73] "9007 Series/Spartan SIP Reed Relays," *Coto Technology*. [Online]. Available: http://cotorelay.com/product/9007-series-spartan-sip-reed-relays/. [Accessed: 07-Sep-2016].

[74] "Resistivity Measurements of Semiconductor Materials using the 4200A-SCS Parameter Analyzer and a Four-Point Collinear Probe". [Online]. Available: http://www.tek.com/dl/1KW-60640-0_FourPointCollinear_4200A-SCS_AN.pdf [accessed on 30 October 2016].

[75] E. Nash, *Common Mode and Instrumentation Amplifiers*. Analog Devices, 1998.

[76] "Arduino - Home." [Online]. Available: https://www.arduino.cc/. [Accessed: 07-Sep-2016].

[77] "KiCad EDA." [Online]. Available: http://kicad-pcb.org/. [Accessed: 07-Sep-2016].

[78] "Open source 4 point probe." [Online]. Available: https://osf.io/kcbmq/. [Accessed: 10-Mar-2017].

[79] "mtu-most/fourpointprobe," *GitHub*. [Online]. Available: https://github.com/mtu-most/fourpointprobe. [Accessed: 10-Mar-2017].

[80] "Java SE | Oracle Technology Network | Oracle." [Online]. Available: http://www.oracle.com/technetwork/java/javase/overview/index.html. [Accessed: 16-Oct-2016].

[81] J. Wren, "WindowBuilder." [Online]. Available: https://eclipse.org/windowbuilder/. [Accessed: 07-Sep-2016].

[82] L. Bárdoš and M. Libra, "Effect of the oxygen absorption on properties of ITO layers," *Vacuum*, vol. 39, no. 1, pp. 33–36, Jan. 1989.

[83] Y. Zhou *et al.*, "Direct correlation between work function of indium-tin-oxide electrodes and solar cell performance influenced by ultraviolet irradiation and air exposure," *Phys. Chem. Chem. Phys.*, vol. 14, no. 34, pp. 12014–12021, Aug. 2012.

[84] I. Gibson, D. W. Rosen, and B. Stucker, *Additive Manufacturing Technologies: Rapid Prototyping to Direct Digital Manufacturing*, 1st ed. Springer Publishing Company, Incorporated, 2009.

[85] T. Wohlers, “Caffery T. Wohlers Report 2015: Additive Manufacturing and 3D Printing State of the Industry: Annual Worldwide Progress Report. Fort Collins: Wholers Associates,” 2015.

[86] R. Jones *et al.*, “RepRap – the replicating rapid prototyper,” *Robotica*, vol. 29, no. 1, pp. 177–191, Jan. 2011.

[87] E. Sells, Z. Smith, S. Bailard, A. Bowyer, and V. Olliver, “RepRap: The Replicating Rapid Prototyper: Maximizing Customizability by Breeding the Means of Production,” Social Science Research Network, Rochester, NY, SSRN Scholarly Paper ID 1594475, May 2010.

[88] A. Bowyer, “3D printing and humanity’s first imperfect replicator,” *3D printing and additive manufacturing*, vol. 1, no. 1, pp. 4–5, 2014.

[89] I. J. Petrick and T. W. Simpson, “3D Printing Disrupts Manufacturing: How Economies of One Create New Rules of Competition,” *Research-Technology Management*, vol. 56, no. 6, pp. 12–16, Nov. 2013.

[90] J. G. Tanenbaum, A. M. Williams, A. Desjardins, and K. Tanenbaum, “Democratizing Technology: Pleasure, Utility and Expressiveness in DIY and Maker Practice,” in *Proceedings of the SIGCHI Conference on Human Factors in Computing Systems*, New York, NY, USA, 2013, pp. 2603–2612.

[91] C. Mota, “The Rise of Personal Fabrication,” in *Proceedings of the 8th ACM Conference on Creativity and Cognition*, New York, NY, USA, 2011, pp. 279–288.

[92] B. T. Wittbrodt *et al.*, “Life-cycle economic analysis of distributed manufacturing with open-source 3-D Printers,” *Mechatronics*, vol. 23, no. 6, pp. 713–726, Sep. 2013.

[93] E. E. Petersen and J. Pearce, “Emergence of Home Manufacturing in the Developed World: Return on Investment for Open-Source 3-D Printers,” *Technologies*, vol. 5, no. 1, p. 7, Feb. 2017.

[94] J. M. Pearce, “Building Research Equipment with Free, Open-Source Hardware,” *Science*, vol. 337, no. 6100, pp. 1303–1304, Sep. 2012.

[95] J. M. Pearce, *Open-Source Lab: How to Build Your Own Hardware and Reduce Research Costs*, 1st ed. Amsterdam: Elsevier Science Publishers B. V., 2013.

[96] T. Baden, A. M. Chagas, G. Gage, T. Marzullo, L. L. Prieto-Godino, and T. Euler, "Open Labware: 3-D Printing Your Own Lab Equipment," *PLOS Biol*, vol. 13, no. 3, p. e1002086, Mar. 2015.

[97] J. M. Pearce, C. M. Blair, K. J. Laciak, R. Andrews, A. Nosrat, and I. Zelenika-Zovko, "3-D Printing of Open Source Appropriate Technologies for Self-Directed Sustainable Development," *Journal of Sustainable Development*, vol. 3, no. 4, p. 17, Nov. 2010.

[98] E. Canessa, C. Fonda, M. Zennaro, and N. DEADLINE, "Low-cost 3D printing for science, education and sustainable development," *Low-Cost 3D Printing*, vol. 11, 2013.

[99] J. M. Pearce, "Applications of open source 3-D printing on small farms," *Organic Farming*, vol. 1, no. 1, pp. 19–35, 2015.

[100] R. Ilardo and C. B. Williams, "Design and manufacture of a Formula SAE intake system using fused deposition modeling and fiber – reinforced composite materials," *Rapid Prototyping Journal*, vol. 16 no. 3, pp. 174-179, Apr. 2010.

[101] C. Newell *et al.*, "Out of bounds additive manufacturing," *Adv. Mater. Process.*, vol. 171, pp. 15–19, 2013.

[102] "3D Printer the large scale printer BigRep ONE," [Online]. Available: https://bigrep.com/bigrep-one/. [Accessed: 12-Feb-2017]

[103] "The Box - The world's biggest 3d printer | BLB Industries." [Online]. Available: http://www.blbindustries.se/the-box.php. [Accessed: 13-Feb-2017].

[104] "HORI 3D Printer Z1000/Z1000D." [Online]. Available: http://www.hori3d.com:81/product-z1000.html. [Accessed: 13-Feb-2017].

[105] "ErectorBot". [Online]. Available: http://www.erectorbot.com/. [Accessed: 13-Feb-2017].

[106] "XceL," *English*. [Online]. Available: https://www.lpfrg.com/en/xcel/. [Accessed: 16-Feb-2017].

[107] "Stratasys IMTS 2016 | Stratasys." [Online]. Available: http://www.stratasys.com/imts2016. [Accessed: 16-Feb-2017].

[108] “AM1 Specifications — Cosine.” [Online]. Available: http://www.cosineadditive.com/am1/. [Accessed: 16-Feb-2017].

[109] “Builder 3D Printers - Quality 3D Printers from the Netherlands,” [Online]. Available: http://builder3dprinters.com/. [Accessed: 16-Feb-2017].

[110] “X1000 3D Printer | German RepRap GmbH.” [Online]. Available: https://www.germanreprap.com/en/products/3d-printer/x1000-3d-printer/. [Accessed: 16-Feb-2017].

[111] “fouche3dprinting,” [Online]. Available: https://www.fouche3dprinting.com. [Accessed: 25-Feb-2017].

[112] “Excel Series 3D Printer Machines - 3D Platform.” [Online]. Available: https://3dplatform.com/products-3/excel-series-3d-printer-machines/. [Accessed: 25-Feb-2017].

[113] “ProtoCentre 1M” [Online]. Available: http://www.aha3d.in/product-2.php. [Accessed: 25-Feb-2017].

[114] “The Cronus | Multi-head 3D Printing Technology | Titan Robotics,” [Online]. Available: http://www.titan3drobotics.com/the-cronus/. [Accessed: 25-Feb-2017].

[115] “BAAM 3D Printed Projects” [Online]. Available: http://wwwassets.e-ci.com/PDF/Products/baam-3d-printed-projects-sheet.pdf. [Accessed: 02-Mar-2017].

[116] L. Li *et al.*, “Big Area Additive Manufacturing of High Performance Bonded NdFeB Magnets,” *Scientific Reports*, vol. 6, p. 36212, Oct. 2016.

[117] G. Rundle, *A Revolution in the Making*. Simon and Schuster, 2014.

[118] G. C. Anzalone, B. Wijnen, and J. M. Pearce, “Multi-material additive and subtractive prosumer digital fabrication with a free and open-source convertible delta RepRap 3-D Printer,” *Rapid Prototyping Journal*, vol. 21, no. 5, pp. 506–519, Aug. 2015.

[119] A. Ferreira, K. M. Arif, S. Dirven, and J. Potgieter, “Retrofitment, open-sourcing, and characterisation of a legacy fused deposition modelling system,” *Int J Adv Manuf Technol*, pp. 1–11, Nov. 2016.

[120] “CNCRouterParts.” [Online]. Available: http://www.cncrouterparts.com/. [Accessed: 02-Mar-2017].

[121] A. K. Johnson, “Linear guide device,” US9175724 B2, 03-Nov-2015.

[122] “Volcano.” [Online]. Available: http://e3d-online.com/E3D-v6/Volcano. [Accessed: 02-Mar-2017].

[123] “BeagleBoard.org - green.” [Online]. Available: https://beagleboard.org/green. [Accessed: 02-Mar-2017].

[124] “GitHub - mtu-most/franklin: 3D printer controlling software.” [Online]. Available: https://github.com/mtu-most/franklin. [Accessed: 02-Mar-2017].

[125] B. Wijnen, G. C. Anzalone, A. S. Haselhuhn, P. G. Sanders, and J. M. Pearce, “Free and Open-source Control Software for 3-D Motion and Processing,” *Journal of Open Research Software*, vol. 4, no. 1, Jan. 2016.

[126] “Debian -- The Universal Operating System.” [Online]. Available: https://www.debian.org/. [Accessed: 14-Mar-2017].

[127] J. W. Comb, W. R. Priedeman, and P. W. Turley, “FDM technology process improvements,” presented at the Proceedings of Solid Freeform Fabrication Symposium, 1994, pp. 42–49.

[128] Thingiverse.com, “Box Vase 5 by David_Mussaffi.” [Online]. Available: http://www.thingiverse.com/thing:268427. [Accessed: 16-Mar-2017].

[129] Thingiverse.com, “Spiral Vase by BigBadBison.” [Online]. Available: http://www.thingiverse.com/thing:570288. [Accessed: 16-Mar-2017].

[130] Thingiverse.com, “Twisted 6-sided Vase Basic by MaakMijnIdee.” [Online]. Available: http://www.thingiverse.com/thing:18672. [Accessed: 16-Mar-2017].

[131] Thingiverse.com, “Koch Snowflake Vase 1 by sphynx.” [Online]. Available: http://www.thingiverse.com/thing:35246. [Accessed: 16-Mar-2017].

[132] C. Zhang, B. Wijnen, and J. M. Pearce, “Open-Source 3-D Platform for Low-Cost Scientific Instrument Ecosystem,” *Journal of Laboratory Automation*, vol. 21, no. 4, pp. 517–525, Aug. 2016.

[133] “MOST Delta Users - Google Groups.” [Online]. Available: https://groups.google.com/a/mtu.edu/forum/?hl=en#!forum/most-delta-users-l. [Accessed: 14-Mar-2017].

[134] “Using Franklin on a CNC Router Parts 3-D printer - Appropedia: The sustainability wiki.” [Online]. Available:

http://www.appropedia.org/Using_Franklin_on_a_CNC_Router_Parts_3-D_printer. [Accessed: 05-Apr-2017].

[135] "Instructions & Configuration | CNCRouterParts." [Online]. Available: http://www.cncrouterparts.com/instructions-configuration-c-44_37.html?osCsid=ev47m8les5iu5qp3qprip2op04. [Accessed: 14-Mar-2017].

[136] "Using Franklin on a CNC Router Parts 3-D Printer - Appropedia: The sustainability wiki." [Online]. Available: http://www.appropedia.org/Using_Franklin_on_a_CNC_Router_Parts_3-D_printer. [Accessed: 16-Mar-2017].

[137] "Athena Software - Appropedia: The sustainability wiki." [Online]. Available: http://www.appropedia.org/Athena_Software. [Accessed: 14-Mar-2017].

[138] K. P. Karunakaran, S. Suryakumar, V. Pushpa, and S. Akula, "Retrofitment of a CNC machine for hybrid layered manufacturing," *Int J Adv Manuf Technol*, vol. 45, no. 7–8, pp. 690–703, Dec. 2009.

[139] C. Baechler, M. DeVuono, and J. M. Pearce, "Distributed recycling of waste polymer into RepRap feedstock," Rapid Prototyping Journal, vol. 19, no. 2, pp. 118–125, Mar. 2013.

[140] G. Braanker, J. Duwel, J. Flohil, and G. Tokaya, "Developing a plastics recycling add-on for the RepRap 3D printer," *Delft University of Technology, Prototyping Lab*, 2010.

[141] "Felfil | Filament maker for 3D printers." [Online]. Available: https://felfil.com/. [Accessed: 14-Mar-2017].

[142] "Universal pellet extruder UPE3D2.0 by mahor - Thingiverse." [Online]. Available: http://www.thingiverse.com/thing:1847917. [Accessed: 14-Mar-2017].

[143] "Arduino Mega Pololu Shield - RepRapWiki." [Online]. Available: http://reprap.org/wiki/Arduino_Mega_Pololu_Shield. [Accessed: 14-Mar-2017].

[144] A. Laplume, G. C. Anzalone, and J. M. Pearce, "Open-source, self-replicating 3-D Printer factory for small-business manufacturing," *Int J Adv Manuf Technol*, vol. 85, no. 1–4, pp. 633–642, Jul. 2016.